

EDITORIAL - Preface to Volume 14 Issue 2 of the Scientific Journal of Civil Engineering (SJCE)

Gjorgji Gjorgjiev EDITOR - IN - CHIEF

Dear Readers,

It is our pleasure to present the second issue of Volume 14 of the *Scientific Journal of Civil Engineering (SJCE)*, continuing the journal's commitment to the dissemination of scientific and professional achievements across the broad field of civil engineering.

The *Scientific Journal of Civil Engineering* provides an international platform for researchers, academics and professionals to exchange knowledge, present original research and contribute to the advancement of contemporary civil engineering. Through its open-access publishing model and rigorous peer-review process, the journal seeks to promote high-quality research and encourage the exchange of knowledge between the scientific community and engineering practice.

This issue comprises five research papers addressing diverse topics of current relevance to civil engineering. The contributions reflect the interdisciplinary character of the profession, ranging from energy performance and economic aspects of buildings to transportation safety, concrete structures and structural engineering.

The first paper investigates the validation of energy simulation models through comparison with actual energy consumption in buildings, highlighting the importance of reliable modelling approaches for evaluating building energy performance. The second contribution examines the cost structure of residential buildings with reinforced concrete structural systems, providing insight into the distribution and significance of construction costs.

The application of contemporary computational methods is represented by a study employing machine learning to identify key risk factors associated with traffic accidents, demonstrating the growing potential of data-driven approaches in transportation engineering and safety analysis. Another contribution addresses the harmonization of design procedures for concrete pavements and industrial floor slabs in the context of EN 206, Eurocode 2 and national regulations, emphasizing the importance of consistency between European standards and engineering practice.

The issue concludes with a numerical seismic analysis of the main girder of a double-girder bridge crane, contributing to the understanding of the structural response of industrial structures under seismic loading.

Together, these contributions illustrate the diversity of challenges currently addressed within civil engineering and the increasing integration of numerical modelling, data-driven methods, sustainability considerations and contemporary standards into engineering research and practice.

On behalf of the Editorial Board, we would like to express our sincere gratitude to the authors for choosing the *Scientific Journal of Civil Engineering* as a platform for presenting their research, and to the reviewers for their valuable expertise, time and commitment throughout the peer-review process.

We hope that the papers presented in this issue will provide useful insights, stimulate further research and encourage continued exchange of knowledge within the civil engineering community.

Sincerely,

(HANDMADE SIGNATURE)

Gjorgji Gjorgiev, Editor-in-Chief

December 2025

SJCE
SCIENTIFIC JOURNAL OF CIVIL ENGINEERING

Impressum

FOUNDER AND PUBLISHER

Faculty of Civil Engineering
Partizanski odredi 24, 1000 Skopje, N. Macedonia

PRINT

This Journal is printed in Geteo print DOOEL Skopje

EDITORIAL OFFICE

Faculty of Civil Engineering
Partizanski odredi 24, 1000 Skopje, N. Macedonia
tel. +389 2 3116 066
fax. +389 2 3118 834
prodekan.nauka@gf.ukim.edu.mk

EDITOR IN CHIEF

Prof. PhD **Gjorgji Gjorgjiev**

Ss. Cyril and Methodius University in Skopje
Faculty of Civil Engineering
Partizanski odredi 24, 1000 Skopje, N. Macedonia
v.vitanov@gf.ukim.edu.mk

EDITORIAL ADVISORY BOARD

Denis Popovski, PhD

Professor, Ss. Cyril and Methodius University in Skopje, Faculty of Civil Engineering, Skopje, N. Macedonia

Jovan Br. Papic, PhD

Professor, Ss. Cyril and Methodius University in Skopje, Faculty of Civil Engineering, Skopje, N. Macedonia

Milica Jovanoska, PhD

Assistant professor, Ss. Cyril and Methodius University in Skopje, Faculty of Civil Engineering, Skopje, N. Macedonia

ISSN: 1857-839X
DOI: 10.55302/SJCE

TECHNICAL EDITORS

Natasha Malijanska Andreevska, PhD

Assistant professor, Ss. Cyril and Methodius University in Skopje, Faculty of Civil Engineering, Skopje,
N. Macedonia

Ivona Nedevska Trajkova, PhD

Assistant professor, Ss. Cyril and Methodius University in Skopje, Faculty of Civil Engineering, Skopje,
N. Macedonia

Frosina Panovska Georgievska, PhD

Assistant, Ss. Cyril and Methodius University in Skopje, Faculty of Civil Engineering, Skopje,
N. Macedonia

EDITORIAL BOARD

Marijana Lazarevska, PhD

Ss. Cyril and Methodius University in Skopje, Faculty of Civil Engineering, Skopje,
N. Macedonia

Elena Dumova Jovanoska, PhD

Ss. Cyril and Methodius University in Skopje, Faculty of Civil Engineering, Skopje,
N. Macedonia

Zlatko Bogdanovski, PhD

Ss. Cyril and Methodius University in Skopje, Faculty of Civil Engineering, Skopje,
N. Macedonia

Ljupco Dimitrievski, PhD

Ss. Cyril and Methodius University in Skopje, Faculty of Civil Engineering, Skopje,
N. Macedonia

Zlatko Zafirovski, PhD

Ss. Cyril and Methodius University in Skopje, Faculty of Civil Engineering, Skopje,
N. Macedonia

Katerina Donevska, PhD

Ss. Cyril and Methodius University in Skopje, Faculty of Civil Engineering, Skopje, N. Macedonia

Tina Dasic, PhD

University of Belgrade, Faculty of Civil Engineering, Belgrade,
R. Serbia

Vlastimir Radonjanin, PhD

University of Novi Sad, Faculty of Technical Sciences, Novi Sad,
R. Serbia

Nenad Ivanisevic, PhD

University of Belgrade, Faculty of Civil Engineering, Belgrade,
R. Serbia

Milos Knezevic, PhD
University of Montenegro, Faculty of Civil Engineering, Podgorica, Montenegro

Marina Rakocevic, PhD
University of Montenegro, Faculty of Civil Engineering, Podgorica, Montenegro

Stjepan Lakusic, PhD
University of Zagreb, Faculty of Civil Engineering, Zagreb, Croatia

Andrej Kryzanowski, PhD
University of Ljubljana, Faculty of Civil and Geodetic Engineering, Ljubljana, Slovenia

Ales Znidaric, PhD
ZAG – Slovenian National Building and Civil Engineering Institute, Ljubljana, Slovenia

Heinz Brandl, PhD
Vienna University of Technology, Institute for Geotechnics, Vienna, Austria

Resat Ulusay, PhD
Hacettepe University, Faculty of Engineering, Ankara, Turkey

SJCE
SCIENTIFIC JOURNAL OF CIVIL ENGINEERING

Impressum

Marc Morell
Institute des Sciences de l'Ingénieur de Montpellier, France

Joost C. Walraven, PhD
Delft University of Technology, Department of Civil Engineering, Delft, Netherlands

Massimo Fragiacomo, PhD
University of L'Aquila, Department of Civil, Construction-Architectural & Environmental Engineering, L'Aquila, Italy

Rita Bento, PhD
Instituto Superior Técnico, Universidade de Lisboa, Department of Civil Engineering, Architecture and Georesources, Lisbon, Portugal

Maosen Cao, PhD
Hohai University, Department of Engineering Mechanics, Nanjing, China

Michael Havbro Faber, PhD
Aalborg University, Department of Civil Engineering, Aalborg, Denmark

Peter Mark, PhD
Ruhr University, Faculty of Civil and Environmental Engineering, Bochum, Germany

Tomas Hanak, PhD
Brno University of Technology, Faculty of Civil Engineering, Brno, Czech Republic

ORDERING INFO

SJCE is published bi-annually. All articles published in the journal have been reviewed.

Edition: 100 copies

SUBSCRIPTIONS

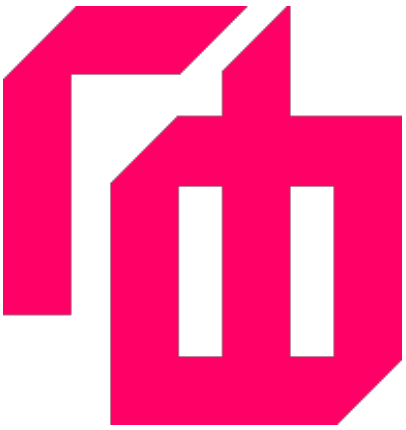
Price of a single copy: for Macedonia (500 den); for abroad (10 EUR + shipping cost).

BANKING DETAILS (NORTH MACEDONIA)

Narodna banka na RNM
Account number: 160010421978815, Prihodno konto 723219, Programa 41

BANKING ETAILS (INTERNATIONAL)

Correspond bank details:
Deutsche Bundesbank
Zentrale Address: Wilhelm Epstein Strasse 14 Frankfurt am Main, Germany SWIFT BIC: MARK DE FF
Bank details:
National Bank of the RNM
Address: Kompleks banki bb 1000 Skopje, North Macedonia
SWIFT BIC: NBRM MK 2X
IBAN: MK 07 1007 0100 0036 254
Name: Gradezen Fakultet, Skopje



СЕКОГАШ БИДИ ИН

WWW.GF.UKIM.EDU.MK

SJCE
SCIENTIFIC JOURNAL OF CIVIL ENGINEERING

CONTENTS

A. Vasileva Ljubotenska, K. Jakimovska, A. Bogdanovic, K. Edip

NUMERICAL SEISMIC ANALYSIS OF THE MAIN GIRDER OF A DOUBLE-GIRDER BRIDGE CRANE 7

M. Matić, M. Šešlija, J. Br. Papić

HARMONIZATION OF DESIGN PROCEDURES FOR CONCRETE PAVEMENTS AND INDUSTRIAL FLOOR SLABS IN THE CONTEXT OF EN 206, EC 2 AND NATIONAL REGULATIONS 15

R. Ristov

IDENTIFICATION OF KEY RISK FACTORS FOR TRAFFIC ACCIDENTS USING MACHINE LEARNING 23

V. Zileska Panchovska, T. Samardzioska, S. Abazi, E. Ajdinoski

COST STRUCTURE FOR RESIDENTIAL BUILDINGS WITH REINFORCED CONCRETE STRUCTURAL SYSTEM 31

L. Dimevska Sofronievska, D. Nikolovski, B. Karanakov

VALIDATION OF ENERGY SIMULATION MODELS THROUGH COMPARISON WITH ACTUAL ENERGY CONSUMPTION IN BUILDINGS 37

Seminar on topic: Application Of Advanced Methods In Dam Engineering - From Digital Twins to Machine Learning

Agenda

09:00h - 10:00h Registration of participants

10:00h - 10:30h Opening of the seminar

10:30h - 12:45h Work session no. 1

1. Application of a Digital Twin to assess the stability of the heightening of combined tailings dam during the service period of the Tailings Storage Facility
Prof. Ljupcho Petkovski, PhD, SCMU, Faculty of Civil Engineering Skopje

2. Creation of digital twin for analysis of the structural stability of the concrete dams - occurence, evolution, concept and application
Prof. Stevcho Mitovski, PhD, SCMU, Faculty of Civil Engineering Skopje

3. Technical moniting of dams in Electro Power Company and data analysis
Slavko Milevski, MSc, AD ESM

4. Artificial Neural Networks - conceptual setup and application in civil engineering
Prof. Marijana Lazarevska, PhD, SCMU, Faculty of Civil Engineering Skopje

12:45h - 13:00h Coffee break

13:00h - 15:15h Work session no. 2

5. Application of Machine Learning Techniques for Inflow Forecasting and Optimal Reservoir Management
Prof. Tina Dašić, PhD, University in Belgrade, Faculty of Civil Engineering

6. From tokens to decisions: understanding and applying large language models in dam engineering
Prof. Fernando Salazar Gonzales, PhD, The International Centre for Numerical Methods in Engineering - CIMNE, Universitat Politècnica de Catalunya BarcelonaTech

7. Machine Learning for Dam Monitoring and Safety Assessment: Pore Pressure Prediction, Sensor Data Reconstruction and Scenario Ánalysis
Assoc. prof. Milica Marković, PhD, University in Nis, Faculty of Civil Engineering and Architecture

8. Machine Learning in Dam Engineering - aspects of possibilities and limitations explored through case studies
Assist. Frosina Panovska Georgievska, MSc, SCMU, Faculty of Civil Engineering Skopje

15:15h - 16:00h Coctail

Chamber of certified architects and certified engineers, Skopje

16th September, 2026

Macedonian Committee on Large Dams

Chamber of Certified Architects and Certified Engineers

NUMERICAL SEISMIC ANALYSIS OF THE MAIN GIRDER OF A DOUBLE-GIRDER BRIDGE CRANE

Anita Vasileva Ljubotenska
MSc, Teaching Assistant
Ss. Cyril and Methodius University in Skopje
Faculty of Mechanical engineering - Skopje
North Macedonia
anita.vasileva@mf.edu.mk
0000-0002-0755-4773

Kristina Jakimovska
PhD, Professor
Ss. Cyril and Methodius University in Skopje
Faculty of Mechanical engineering - Skopje
North Macedonia
0000-0002-5629-359X

Aleksandra Bogdanovic
PhD, Professor
Ss. Cyril and Methodius University in Skopje
Institute of Earthquake Engineering and Engineering Seismology
North Macedonia
0000-0001-6710-3248

Kemal Edip
PhD, Professor
Ss. Cyril and Methodius University in Skopje
Institute of Earthquake Engineering and Engineering Seismology
North Macedonia
0000-0002-4542-8911

Received: 11.12.2025
Accepted: 22.01.2026
Published: 26.01.2026

DOI: 10.55302/SJCE2514207vlj

In this paper a numerical analysis of a double-girder bridge crane was carried out in order to evaluate the seismic response of the main girder. The analysis includes static, modal and transient FEM analyses in Ansys, with the aim of obtaining a realistic picture of the structural behavior under earthquake excitation. Through the static analysis, the reference values for stresses and deformations under working conditions were obtained, while the modal analysis identified the natural frequencies and the dominant vibration modes. The transient analysis, performed with the real earthquake record El Centro, provides the time histories of displacements, accelerations and stresses at characteristic points along the span. The results showed that the seismic excitation causes increased and time-variable responses compared to the static values, but the structure remained in the elastic domain. The applied approach enables a more detailed representation of the dynamic effects on the girder and serves as a basis for more detailed inspection control of bridge cranes.

Keywords: bridge crane, main girder, modal analysis, transient analysis, Ansys

1. INTRODUCTION

In industry, cranes are used for most processes, and in the largest percentage bridge cranes are applied. The condition of bridge cranes is essential both for safe operation and for the overall efficiency of the production process. In order to perform inspection, maintenance and proper use of cranes, it is necessary to apply a series of standards, regulations and laws [1, 2]. In our country, there is a Regulation for the use of cranes and industrial transporters, as well as a Law on technical inspection [3], [4], [5]. The regulation and the law define guidelines for inspection procedures, inspection intervals and the

Scientific Journal of Civil Engineering (SJCE)
© 2025 by Faculty of Civil Engineering, SCMU - Skopje is licensed under CC BY-SA 4.0

required documentation. However, in the current national regulation for cranes in the Republic of North Macedonia there is no explicit requirement for performing detailed seismic analysis of bridge cranes, as is the case for building structures according to Euro code 8. Although seismologically North Macedonia belongs to a zone of moderate to high seismic activity, as part of the South-European–Mediterranean seismic belt, seismic requirements for bridge cranes remain insufficiently addressed in national technical regulations. Bridge cranes, which are almost an inseparable part of every industrial facility, contain moving elements, contact surfaces and masses that are not rigidly connected to the main structure [9], [10], [11]. This makes them more sensitive to earthquake excitation and requires detailed analysis to ensure safe operation under extreme conditions [12-14].

The need for such research is supported by a review of previous studies in the fields of crane engineering reliability, assessment, maintenance, regulations and standards for crane use, as well as seismology research on the Balkans.

From the literature review [1], [2], [6], [7], [8] it is evident that bridge cranes are widely used, and the main girder represents their most loaded element, directly affecting the load-carrying capacity and safety of the crane. The national regulation [1], [2] covers technical inspection procedures, but at no point requires mandatory seismic analysis of bridge cranes. On the other hand, studies [9], [10], [11], [12] point out that the Balkans represent one of the most active seismic regions in Europe, with a total of 15,417 earthquakes recorded on the territory of North Macedonia in the period 2010–2021 [9]. Previous research indicates that bridge cranes may exhibit significant nonlinear behavior during earthquakes, as a result of their structural configuration [13-18].

Study [13] presents a methodology for simulating bridge cranes under seismic loading based on the SOCRAT benchmark. The models are calibrated with experimental results and later used for blind nonlinear predictions under high seismic intensities. The approach uses shell elements for the crane structure, connector elements for rail interaction with frictional behavior, and an explicit dynamic procedure for severe earthquakes. Research [14] focuses on the static and dynamic stability of tower cranes, emphasizing their sensitivity to destabilizing effects such as wind and seismic actions. Stability is identified as a key parameter in crane design, especially for tall and flexible systems. In [15], a numerical reliability assessment of pre-stressed concrete bridges is performed through time-domain analysis with material nonlinearity. The study shows that damping and earthquake parameters (PGA, magnitude) significantly influence reliability, while geometric variations have a smaller effect. Study [16] investigates the vertical seismic response of equipment with low vertical stiffness, using a 150-ton overhead crane as an example. Scale-model tests and nonlinear time-history analyses show strong amplification of the vertical response, with numerical results closely matching experiments. Research [17] analyzes the influence of overhead cranes with a hanging load on precast industrial buildings during the 2012 Emilia earthquake sequence. Simplified and 3D nonlinear analyses reveal that parameters such as damping, rope length and structural ductility affect roof displacements and horizontal forces transmitted by the crane. Study [18] examines the nonlinear seismic behavior of a steel warehouse equipped with an overhead crane. Using pushover and time-history analyses with Chilean earthquake records, the authors conclude that crane loads do not significantly affect the global seismic performance of the warehouse, although directional ductility varies. More recent work emphasizes FEM-based structural optimization. Study [19] applies analytical calculations and finite element analysis to optimize girder cross-sections, reducing unit weight without compromising structural capacity. In [20, numerical analysis of an EOT crane girder is carried out to evaluate deflections under rated loads. Results confirm that girder deformations remain within allowable limits, validating the structural design. Research [21] models a bridge crane structure in ABAQUS and analyzes stresses and displacements under typical operating conditions. Comparison between theoretical and FEM results highlights the higher accuracy and practical value of FEM for crane design. Finally, study [22] compares analytical and numerical results for a single-girder crane using Catia and Ansys. The FEM analysis produces slightly lower but consistent results relative to analytical calculations, demonstrating the reliability of numerical simulations for main girder evaluation.

Overall, the literature review showed that although the country belongs to a seismically active region, there are very few studies related to seismic analyses of bridge cranes, especially in the Balkans, which is the second most

seismically active region in the world after the Pacific "Ring of Fire."

2. METODOLOGY

The methodological approach in this paper is based on integrating static, modal, and transient numerical analyses to evaluate the seismic response of the crane's main girder. The static results from Ansys Workbench and the dynamic results from Ansys Mechanical APDL are used jointly to identify critical regions and assess structural behavior under earthquake loading [23], [24]. A real ground-motion record (El Centro) [25] is applied in the transient analysis, while the modal results support the understanding of the girder's dynamic sensitivity. The phases of the research are presented in Figure 1.

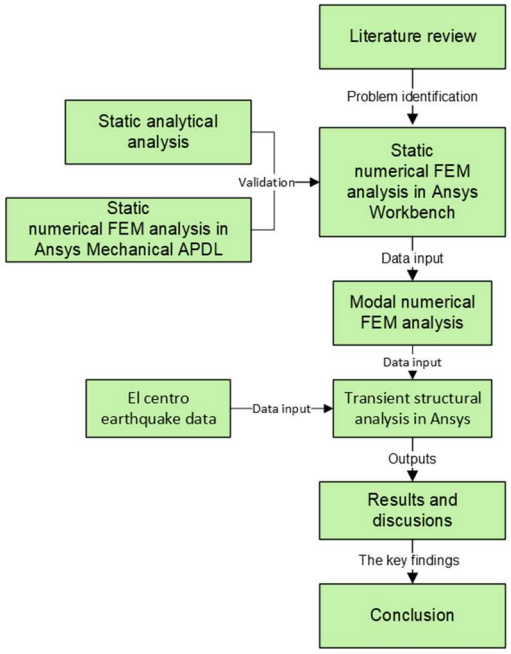


Figure 1. Methodology flowchart

3. NUMERICAL ANALYSIS

In this study, static, modal and transient dynamic analyses were performed in Ansys on the main girder located at the Institute of Earthquake Engineering & Engineering Seismology – IZIIS. The main girder of the bridge crane is a welded box profile, and its geometry and material properties were taken from the crane documentation (Table 1) [6]. Before the static analysis, a numerical analytical calculation was carried out, from which it was obtained that the maximum moment occurs at approximately 12.8 m from the left support and is about $M_{max} \approx 150$ kNm, while the bending stress is $\sigma_{max} \approx 99$ MPa. The analytical results serve as a basis for verification with the numerical analysis.

Table 1. Geometrical characteristics and exploitation parameters of the main girder

Characteristics / Parameters	Symbol	Value
Height of the girder	H	700 mm
Width of the girder	B	450 mm
Thickness of top/bottom plate	T	8 mm
Thickness of side plates	S1, S2	6 mm
Lifting capacity	Q	10 t
Span	L	16.24 m
Lifting height	H	9 m
Material	S235JR	
Elastic modulus	E	2.10×10^{11} Pa
Poisson's ratio	v	0.30
Density	ρ	7850 kg/m³
Yield strength	fy	235 MPa
Stressallow	σ_{allow}	≈ 0.6·fy = 141 MPa

3.1. STATIC ANALYSIS

The CAD model created in SolidWorks was transferred into ANSYS Workbench [24], [25]. The CAD model of the main girder is shown in Figure 2.



Figure 2. CAD model of the double-girder main girder

In the numerical simulation, the girder is treated as a simply supported beam, with one end vertically fixed and the other axially movable (Figure 3). The mesh is denser in the zones where stress concentrations are expected, around the supports and the trolley path, and coarser in the remaining parts. A mesh density check was performed, where further refinement did not produce stress variations greater than σ < 3%. This confirmed that the selected mesh was appropriate. Additionally, before performing the dynamic simulations, a static analysis was also carried out in Ansys Mechanical APDL for verification. The main girder was represented with a beam element (sectype, 1, beam, hrec), unlike the detailed 3D SolidWorks model in Ansys Workbench. The results showed an expected difference of around 10%, which is typical when comparing a simplified beam model created in Ansys Mechanical APDL with a full 3D model created in SolidWorks. The difference occurs because the beam model in APDL represents an idealized line geometry and therefore does not capture the local stress concentrations that are visible in the detailed 3D solid model in Workbench.

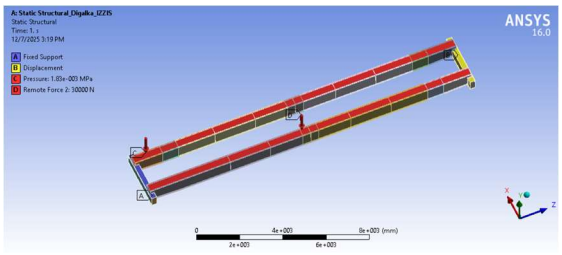


Figure 3. Static FE model with boundary conditions and mid-span load

3.2. MODAL ANALYSIS

The modal analysis was performed in ANSYS Mechanical APDL to determine the natural frequencies and mode shapes required for the dynamic evaluation. The same structural model and boundary conditions from the static analysis were used. The eigenvalue extraction was carried out with the LANB solver, requesting the first ten modes. Mode shapes were visualized using the SET and PLDISP commands, ensuring proper identification of the dominant vibration patterns needed for the subsequent transient analysis.

3.3. TRANSIENT ANALYSIS

The transient analysis was performed in ANSYS Mechanical APDL by applying the El Centro ground-motion record [25], scaled to 0.25 g and with a total duration of 10 s (Figure 4).

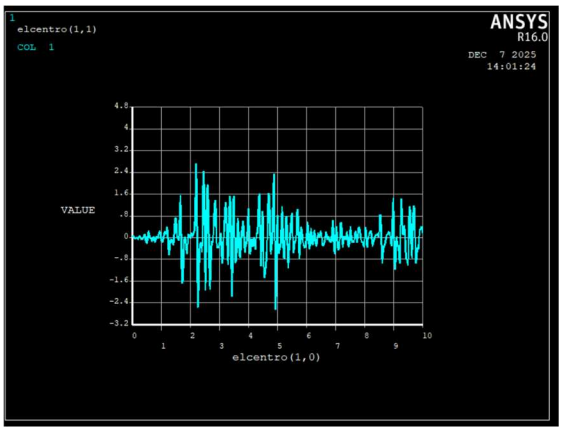


Figure 4. Input ground acceleration record (El Centro, 0.25 g)

Rayleigh damping was introduced with coefficients α = 1.277323 and β = 0.00178225, and the equations of motion were solved with a full direct integration scheme, using a constant time step of Δt = 0.02 s. The ground acceleration was applied as a vertical base excitation following an initial gravity step, while the vertical and horizontal displacements, accelerations, and equivalent (von Mises) stresses were monitored at three characteristic nodes along the main girder (left support, mid-span, and right support). The locations of the selected monitoring nodes are shown in Figure 5. The obtained time-history results were subsequently compared with the static response in order to assess the influence of seismic loading on the overall structural behavior.

Table 2. Basic transient-analysis parameters

Parameter	Value
Earthquake record	El Centro (0.25 g)
Total duration	10 s
Time step Δt	0.02 s
Damping (Rayleigh)	α = 1.277323, β = 0.00178225
Beam element	BEAM188
Mesh size	0.20 m
Output nodes	Left support, mid-span, right support

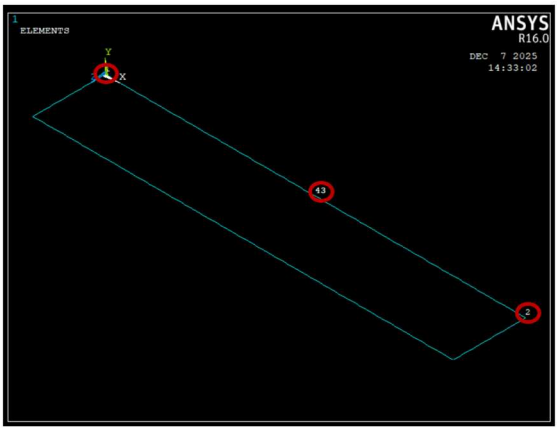


Figure 5. Selected monitoring nodes along the main girder used in the transient analysis

4. RESULTS AND DISCUSSION

4.1. STATIC ANALYSIS RESULTS AND DISCUSSION

In this study, only the simulations with the load positioned at mid-span are included, because the analytical calculation showed that the maximum stress occurs at that location. When the trolley is located at mid-span, the maximum stress is 155.59 MPa, while the deformation is 4.42 mm (Figure 6). From the figures (Figure 7), it can be seen that these are local stresses occurring at certain points of the girder, while the remaining part of the girder is subjected to stresses below the allowable limit (141 MPa).

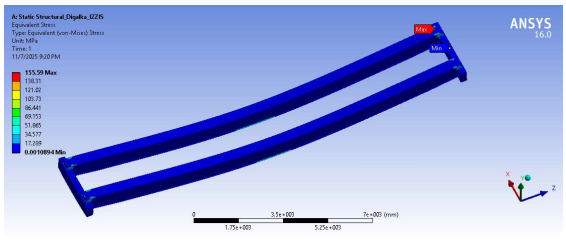


Figure 6. Equivalent von Mises stress distribution under static loading at mid-span

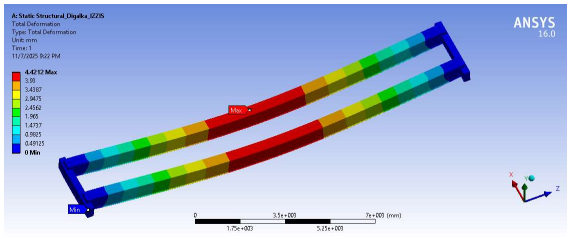


Figure 7. Total deformation of the main girder under static loading at mid-span

4.2. MODAL ANALYSIS RESULTS AND DISCUSSION

The first several modes exhibited near-zero frequencies, corresponding to rigid-body motions, while the first significant bending mode occurred at 0.66 Hz, followed by higher-order modes at 3.76 Hz and 4.05 Hz. These values indicate a flexible structural response, typical for long-span girders, and provide the basis for the subsequent transient seismic analysis. The extracted modal frequencies are summarized in Table 3. In Ansys, the deformed shape of the structure was obtained at a frequency of 3.76 Hz, which represents the dominant bending mode (Figure 8). This modal shape was essential for understanding the dynamic sensitivity of the girder and served as the basis for an accurate transient seismic analysis. The second vibration mode, obtained at a frequency of 4.05 Hz, exhibits a higher-order bending deformation along the girder span (Figure 9). Compared to the first mode, this mode involves more complex curvature and provides insight into the dynamic flexibility of the structure. These modal characteristics are essential for understanding the girder's response under seismic excitation.

Table 3. Natural frequencies of the crane girder

Mode	Frequency [Hz]	Mode direction
1	0.66	Vertical bending
2	3.76	Vertical bending
3	4.05	Vertical bending

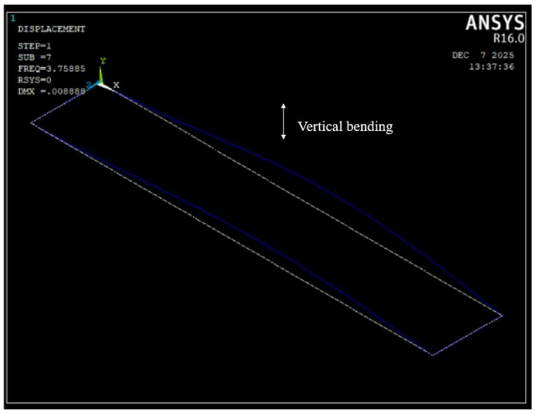


Figure 8. First vibration mode of the crane girder (f = 3.76 Hz)

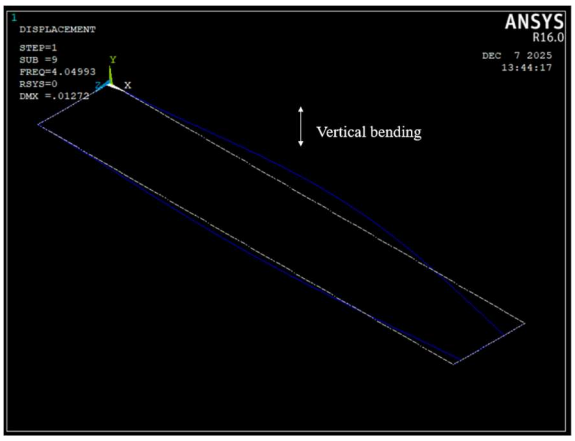


Figure 9. Second vibration mode of the crane girder (f = 4.05 Hz)

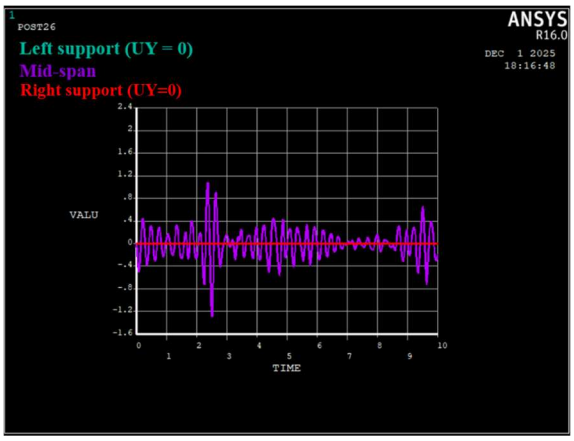


Figure 10. Time history of the vertical displacement UY at the three monitoring nodes (left support and right support UY=0)

4.3. TRANSIENT ANALYSIS AND DISCUSSION

The transient analysis performed using the El Centro earthquake record (0.25 g) showed that the dynamic response of the main girder is significantly more intense and time-dependent compared to the static cases. The largest vertical displacements and accelerations occur at the mid-span node (node 43), which is consistent with the expected behavior of a simply supported beam subjected to oscillatory excitation.

The time history of the vertical displacement UY at the mid-span shows several pronounced peaks during the strongest pulses of the earthquake, with a maximum negative deformation of approximately –12.88 mm and a maximum positive value of about +10.79 mm (Figure 10). Due to the fixed boundary conditions, no displacements were recorded at the support nodes; therefore, only the mid-span response is visible.

These values are larger than the static displacement but remain within the elastic range of the material. The vertical accelerations reach up to ±9.8 m/s², which is approximately equal to the gravitational acceleration (≈1 g) and indicates significant dynamic excitation.

Therefore, it can be concluded that the structure maintains its load-carrying capacity under the considered seismic excitation. Table 4 presents the extreme values of vertical displacements and accelerations obtained from the transient analysis at the three monitoring nodes.

Table 4. Peak transient response values at monitoring nodes

Node location	Quantity	Min value [mm]	Max value [mm]
Left support	ACCY [m/s²]	0.00	0.00
Mid-span	ACCY [m/s²]	–9.81	8.86
Right support	ACCY [m/s²]	0.00	0.00
Left support	UY [mm]	0.00	0.00
Mid-span	UY [mm]	–12.88	10.79
Right support	UY [mm]	0.00	0.00

Figure 11 shows the contour distribution of the equivalent (von Mises) stresses at the moment of maximum response. It is noticeable that the highest stresses occur near the supports and in the regions where the stiffness of the structure changes, which is typical for bending-loaded girders under dynamic excitation. Although pronounced local peaks are present, the maximum value on the order of $1.13 \cdot 10^8$ Pa (113 MPa) remains below the yield strength of S235JR steel, indicating that the structure stays within the elastic domain even under seismic conditions.

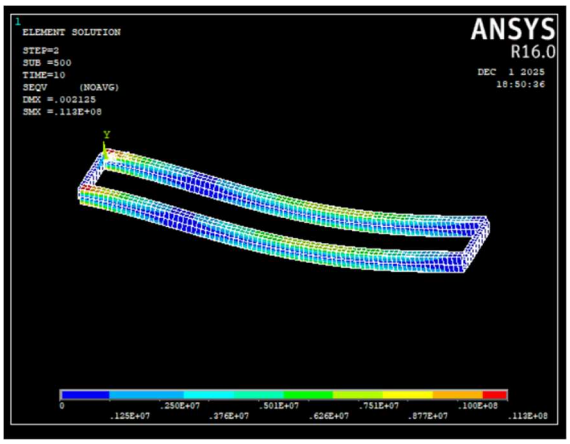


Figure 11. Contour distribution of equivalent (von Mises) stresses at peak seismic response

Based on the obtained results, it can be concluded that the seismic excitation produces a combined bending and inertial response, with momentary peaks that exceed the static behavior. However, the structure remains within the elastic domain and does not show signs of damage under the considered earthquake intensity.

5. CONCLUSION

This study presented a numerical approach for assessing the seismic response of the main girder in a double-girder bridge crane, using static, modal and transient analyses under real earthquake excitation. The static analysis showed that the girder operates within the elastic domain under nominal service loading. The modal analysis identified the dominant natural vibration modes and indicated that the low natural frequencies are characteristic of long and flexible structures, suggesting that dynamic effects can have a significant influence on their behavior during an earthquake.

The transient analysis based on the El Centro earthquake record showed that the largest structural responses occur at mid-span. The maximum vertical displacements reached approximately 10–13 mm, while the equivalent (von Mises) stresses remained below 113 MPa. These results indicate that the structure retains its load-carrying capacity and does not enter the plastic range under the considered seismic intensity.

Overall, the results confirmed that earthquake excitation causes increased deformations compared to static conditions, but the structure remains safe. The analysis shows that static calculations alone are not sufficient for fully understanding the behavior of bridge cranes under seismic loading, and that transient dynamic analyses represent a necessary step for realistic evaluation of their safety and performance. The applied methodology can serve as a basis for future assessments, inspections, and the development of monitoring systems for bridge cranes in seismically active regions.

REFERENCES

[1] Ministry of Labour and Social Policy of the Republic of North Macedonia. (1982). *Rulebook on the Use of Cranes and Industrial Transporters* (Official Gazette of RM No. 10/82; amendment No. 17/91)

[2] Ministry of Economy of the Republic of North Macedonia. (2006). *Law on Technical Requirements for Products and Conformity Assessment* (Official Gazette of RM No. 33/06; amendments No. 63/07, 20/09, 26/12, 23/13, 44/15, 120/18)

[3] Ostrić, D. (2009) Dizalice, Univerzitet u Beogradu, Mašinski fakultet.

[4] Јакимовска, К. (2021). Машини за цикличен транспорт, Универзитет,,Св. Кирил и Методиј" во Скопје, Машински факултет-Скопје.

[5] Институт за стандардизација на Република Македонија. (2015). МКС EN 13001-1: Кранови — Општ дизајн — Дел 1: Општи принципи. ИСРМ

[6] Hoffmann, K., Krenn, E., & Stanker, G. (2004). Fördertechnik: Maschinensätze, Fördermittel, Tragkonstruktionen, Logistik (5th ed., Vol. 2). Oldenbourg.

[7] Hoffmann, K., Krenn, E., & Stanker, G. (2012). Fördertechnik 1: Bauelemente, Konstruktion, Berechnung. Vulkan-Verlag GmbH.

[8] Seeßelberg, C. (2016). Kranbahnen: Bemessung und konstruktive Gestaltung nach Eurocode (5th ed.). DIN Media.

[9] Drogreshka, K., & Najdovska, J. (2021, January). Seismicity in the republic of north macedonia during the period 2010-2020. In Proceedings of the Fourth Congress of the Macedonian Geologists (No. INIS-MK--210001, pp. 65-71).

[10] Drogreshka, K., Najdovska, J., Delipetrev, M., & Delipetrev, M. R. (2024, May). High Seismic Activity of Republic of North Macedonia in the Period 2015–2020. In 12th Congress of the Balkan Geophysical Society (Vol. 2024, No. 1, pp. 1-5). European Association of Geoscientists & Engineers.

[11] Tretyak, K. R., & Brusak, I. (2020). The research of interrelation between seismic activity and modern horizontal movements of the Carpathian-Balkan region based on the data from permanent GNSS stations. Geodynamics, 1, 28.

[12] Baskakova, G. V., Vasilyeva, N. A., Nikishin, A. M., Doronina, M. S., & Ihsanov, B. I. (2022). Identification of the main tectonic events by using 2D–3D seismic data in the eastern Black Sea. Moscow University Geology Bulletin, 77(5), 466-478.

[13] Rodríguez, J., Reboul, J., González, P., Crespo, M., Borgerhoff, M., & Schneeberger, C. (2022). Modelling of an Overhead Crane under Seismic Excitations (SOCRAT).

[14] Potîrniche, A., & Căpățână, G. (2023). Aspects regarding static stability and dynamic stability of the tower cranes. Int. J. Mod. Manuf. Technol, 15(2).

[15] Pourzeynali, S., & Hosseinnezhad, A. (2009). Reliability analysis of bridge structures for earthquake excitations.

[16] Otani, A., Nagashima, K., & Suzuki, J. (2002). Vertical seismic response of overhead crane. Nuclear Engineering and Design, 212(1-3), 211-220.

[17] Belleri, A., Labò, S., Marini, A., & Riva, P. (2017). The influence of overhead cranes in the seismic performance of industrial buildings. Frontiers in Built Environment, 3, 64.

[18] Lisperguier, N., López, Á., & Vielma, J. C. (2023). Seismic performance assessment of a moment-resisting frame steel warehouse provided with overhead crane. Materials, 16(7), 2815.

[19] Albar, Y., & Onur, Y. A. (2023). ANALYTICAL INVESTIGATION AND OPTIMUM DESIGN OF A DOUBLE GIRDER OVERHEAD CRANE. Journal of Mechanical Engineering and Technology (JMET), 15(2), 53-65.

[20] Singh, A. (2022). Analysis of the Crane Girder.

[21] Meng, Z., Yifei, T., & Xiangdong, L. I. (2018). Finite element analysis of bridge crane metal structure based on ABAQUS. In MATEC Web of Conferences (Vol. 198, p. 01004). EDP Sciences.

[22] Molnár, D., Blatnický, M., & Dižo, J. (2022). Comparison of analytical and numerical approach in bridge crane solution. Manuf. Technol. 22 (2)(2022).

[23] Lee, H.-H. (2021). Finite element simulations with ANSYS Workbench 2021: Theory, applications, case studies. SDC Publications.

[24] Kochmann, D. M. (2025). Introduction to finite element analysis. ETH Zurich.

[25] Udwadia, F. E., & Trifunac, M. D. (1973). Comparison of earthquake and microtremor ground motions in El Centro, California. Bulletin of the Seismological Society of America, 63(4), 1227-1253.

Marjan Matić
MSc, Civil Engineer
MHM Projekt d.o.o, Novi Sad
Serbia
marjangrmatic@gmail.com

Miloš Šešlija
PhD, Associate Professor
University of Novi Sad
Faculty of Technical Sciences
Serbia
0000-0002-8857-8952

Jovan Br. Papić
PhD, Professor
Ss. Cyril and Methodius University in Skopje
Faculty of Civil Engineering - Skopje
North Macedonia
0000-0002-2952-302X

HARMONIZATION OF DESIGN PROCEDURES FOR CONCRETE PAVEMENTS AND INDUSTRIAL FLOOR SLABS IN THE CONTEXT OF EN 206, EC 2 AND NATIONAL REGULATIONS

Received: 11.12.2025
Accepted: 26.01.2026
Published: 27.01.2026

DOI: 10.55302/SJCE2514215m

Concrete pavement structures in Serbia and throughout the Western Balkans are still designed according to standards published more than 30 years ago, relying on material models derived from PBAB 87. Industrial floor slabs, although structurally almost identical to concrete pavements, are often designed according to foreign guidelines, using material properties determined in accordance with EN 206 and EC 2. Modern national regulation, including the Regulation on Technical Requirements for Concrete, SRPS EN 206:2021, SRPS U.M1.206:2023, and EC 2, requires a unified approach to defining concrete properties for all concrete structures. As a result, a significant discrepancy arises: structures exhibiting the same mechanical behavior are designed using different material models, with different values of tensile and flexural strength, modulus of elasticity, and compressive strength. This paper provides an overview of current design practice for concrete pavements and industrial floor slabs, with special emphasis on manipulation–traffic slabs used on industrial platforms. Concrete properties according to PBAB 87 / SRPS U.E3.020 are compared with those defined in EN 206 / EC 2, accompanied by a discussion on how this choice affects structural design. Since the second generation of EC 2 does not cover slabs on ground, the need to harmonize national road engineering standards with EN 206 is emphasized, as well as the need for the third generation of Eurocodes to introduce specific provisions for concrete pavements and industrial slabs.

Keywords: Concrete pavement, industrial floor slab, EN 206, Eurocode 2, flexural tensile strength, pavement design

Scientific Journal of Civil Engineering (SJCE)
© 2025 by Faculty of Civil Engineering, SCMU - Skopje is licensed under CC BY-SA 4.0

1. INTRODUCTION

Concrete slabs-on-ground represent a broad group of engineering structures that include road pavement structures, concrete slabs of airport surfaces, as well as industrial floor slabs and manipulation–traffic slabs within logistics, transshipment, and industrial complexes. Whether they are traffic-bearing surfaces exposed to heavy axle loads or industrial platforms intended for truck manoeuvring, forklift operation, and storage of goods, the essential mechanical behaviour of these structures is the same: a cast concrete slab resting on a deformable subgrade and subjected to concentrated, cyclic, and dynamic wheel loads, accompanied by additional effects of temperature gradients, shrinkage, and restrained movements due to friction at the slab–subgrade interface.

Despite the clearly expressed structural similarity, design practice in Serbia and the region has evolved in two separate directions. Concrete pavement structures are still designed according to road engineering standards SRPS U.C4.014 and SRPS U.E3.020, based on the material models originating from PBAB 87. In contrast, industrial floor slabs are most commonly designed according to foreign guidelines where concrete properties are determined in accordance with standards EN 206 and EC2. As a consequence, for structures exhibiting the same mechanical behaviour, different systems of values for tensile strength, flexural strength (modulus of rupture), and modulus of elasticity are often used, resulting in different design outcomes and inconsistencies in engineering practice.

Modern national regulation further emphasises this discrepancy. The Regulation on Technical Requirements for Concrete, together with SRPS EN 206:2021, SRPS U.M1.206:2023, and SRPS EN 13670, prescribes the mandatory application of unified criteria for defining concrete properties and controlling its quality. Eurocode 2 also represents a mandatory basis for the design of all concrete structures, including those exposed to corrosion, frost, chlorides, and abrasion. This indirectly imposes the requirement that both concrete pavements and industrial slabs be designed using the same system of material parameters.

The aim of this paper is to:

- present the existing design practices for concrete pavement structures and industrial floor slabs in domestic and international contexts;
- compare the material models according to PBAB 87 and EN 206/EC 2 used in the design of slabs-on-ground;
- analyse the influence of differences in concrete properties on design results;
- consider the normative implications and the need for harmonizing national standards;
- point out that the 2nd generation of EC2 does not cover slabs-on-ground and propose potentials for development of standardization in this field.

2. EXISTING DESIGN PRACTICES FOR CONCRETE SLABS-ON-GROUND

Concrete slabs-on-ground used in traffic and industrial surfaces are designed based on the stress–strain behaviour of concrete supported by a subgrade defined through the subgrade reaction modulus “k”. Regardless of whether the structure is a pavement slab or an industrial floor, the key mathematical–physical model originates from Westergaard’s theory of an elastic plate on a semi-elastic foundation. However, road engineering practice and industrial practice have developed in different directions and today rely on different sets of standards and material models. The following sections present the actual state of design methodologies, insofar as they are based on SRPS standards and international guidelines such as TR34, ACI 360, and PCA.

2.1 CONCRETE PAVEMENT STRUCTURES ACCORDING TO SRPS U.C4.014 AND SRPS U.E3.020

In Serbia, concrete pavement structures are designed according to the standards U.C4.014 and U.E3.020, which are based on the classical Westergaard theory of a plate on an elastic foundation. Its fundamental assumptions are:

- concrete is idealized as a homogeneous, isotropic, and linear-elastic body of constant thickness;
- the subgrade provides a vertical reaction proportional to the deflection, whereby the reaction per unit area is given by $q = k \cdot w$, where q is the subgrade reaction pressure [kN/m²], k is the modulus of subgrade reaction [kN/m³], and w is the vertical deflection of the slab;

- the subgrade reaction modulus k is treated as a constant (Winkler idealization);
- the load is transferred uniformly over a circular (in the more recent version elliptical or square) contact area when the load acts inside the slab or at a corner, and over a semicircular (semi-elliptical) contact area when the load acts at the slab edge.

In accordance with the classical Westergaard approach, the standards define three characteristic load positions:

- interior loading – wheel load "sufficiently far from the edges" (distance ≥ $l + a$);
- edge loading – load position on the slab edge, sufficiently far from the corner (≥ $l - a$);
- corner loading – point of application in the corner, at a distance ≈ a from both edges.

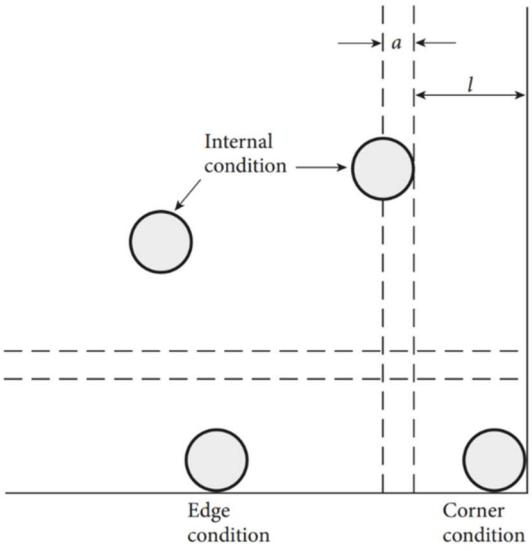


Figure 1. Characteristic load positions

Using Westergaard's method, the following stresses are determined:

- σ_i – interior flexural stresses;
- σ_e – edge flexural stresses;
- σ_c – corner flexural stresses.

These expressions explicitly originate from Westergaard's differential equations for plates on a Winkler foundation and represent the basis of the methodology for designing concrete pavement structures.

The material properties of concrete in these standards are based on the PBAB 87 concrete classes, which include higher values of modulus of elasticity and flexural strength compared to the values defined by EN 206 and Eurocode 2.

2.2 INDUSTRIAL FLOOR SLABS ACCORDING TO TR34, ACI 360 AND PCA

For industrial floor slabs, international methodologies are applied, among which TR34 (Concrete Society), ACI 360R-10, and PCA methods for slabs-on-ground are the most prominent. These guidelines also originate from Westergaard's theory but introduce the modern concept of limit state design (ULS and SLS), as well as a more detailed treatment of contact stresses, storage loads, and load transfer across joints.

The basic elements of the TR34 approach include:

- design of ultimate limit states (ULS) for bending, shear forces, and corner bearing (Meyerhof and Hetenyi);
- serviceability limit states (SLS) covering stress and deformation limitations (Westergaard);
- defining contact areas and pressures depending on the type of industrial vehicle (VNA forklifts, heavy forklifts, low-platform transporters);
- stress calculation for wheel passage across construction, contraction, and expansion joints;
- analysis of the influence of storage loads (rack columns, pallets, containers).

The subgrade reaction modulus in TR34 is determined based on plate load testing or on geotechnical parameters/moduli (Evd, Ed, Ms, E, etc.), with corrections depending on load width and subgrade layering. Fatigue is treated analogously to road engineering methods, through reduction of allowable stresses depending on the number of cycles, without the use of advanced damage models.

Industrial floor slabs are designed using concrete properties defined according to EN 206 and EC 2, including mean and characteristic tensile strength, flexural strength, and modulus of elasticity.

ACI 360R-10 defines industrial floor slabs as slabs on an elastic foundation, with emphasis on selecting the slab type (plain concrete slab, jointed slab, slab with dowels, slab reinforced for crack control). Unlike TR34, the ACI

methodology does not introduce limit state design but uses the allowable stress concept based on Westergaard stress formulas, PCA recommendations, and empirical coefficients. It focuses on:

- determining the minimum slab thickness;
- controlling the width and layout of construction and contraction joints;
- selecting reinforcement for crack control;
- load transfer across joints (dowels).

The ACI 360 approach is more conservative regarding joint width but defines contact stresses and wheel crossing over joints less rigorously compared to TR34.

The Portland Cement Association's (PCA) method represent the oldest classical approach for designing floor slabs and concrete pavement slabs, based exclusively on Westergaard's theory. PCA design provides the minimum slab thickness based on:

- edge, interior, and corner stresses;
- subgrade reaction modulus *k*;
- fatigue calculation through reduction of allowable stresses.

Unlike TR34, PCA does not introduce limit state design nor contact models for modern industrial vehicles, but remains within the domain of classical elastic analysis. In practice, it is still used as a reference for minimum slab thicknesses in the USA and Canada.

2.3 COMPARISON OF DESIGN APPROACHES FOR CONCRETE PAVEMENT STRUCTURES AND INDUSTRIAL FLOOR SLABS

Although the design systems for concrete pavement structures and industrial floor slabs have evolved within different standards and technical guidelines, both approaches are based on the same mechanical foundation—the bending behaviour of an elastic concrete slab supported by a subgrade defined by the subgrade reaction coefficient *k*. The load positions considered in the analysis (interior, edge, and corner loading) and the basic stress expressions derived from Westergaard's theory are common to both methodologies. The differences arise from the following aspects:

- material models: pavement design standards apply values from the PBAB 87 system, whereas industrial floor slab design uses concrete properties according to EN 206 and EC 2;
- types of loading: industrial floor slabs are subjected to additional point and storage loads (forklifts, rack column loads, container units), while pavement structures are predominantly exposed to heavy traffic and environmental effects;
- limit state design: industrial methodologies implement ultimate limit states (ULS) and serviceability limit states (SLS), pavement structures in domestic standards are formally based on limit state theory; however, their practical design is governed primarily by serviceability limit state criteria, where flexural tensile strength is treated as a limiting stress value.

These differences are crucial for understanding inconsistencies in the selection of material models and represent the basis for the analysis presented in the next chapter.

3. MATERIAL MODELS: PBAB VS. EN 206 / EUROCODE 2

The design of concrete slabs-on-ground directly depends on the flexural tensile stress capacity of the concrete slab, the modulus of elasticity of concrete, and the way characteristic and design material parameters are defined. In domestic practice, the standards for designing concrete pavement structures are based on the values from PBAB 87, whereas industrial floor slabs predominantly use values determined according to EN 206 and EC 2. This difference in the selection of material models leads to a inconsistency in the design of structures that are mechanically and functionally similar.

3.1 PROPERTIES OF CONCRETE ACCORDING TO PBAB 87 / SRPS U.E3.020

The PBAB 87 / SRPS U.E3.020 methodology defines concrete grades (from MB 10 to MB 60) through nominal compressive strength, with specified values of modulus of elasticity, tensile strength under axial loading, and flexural tensile stress values obtained empirically:

$$f_{bzm} = 0.25 \cdot \sqrt[3]{f_{bk}^{\,2}} \qquad (1)$$

where:

f_{bzm} –mean value of concrete tensile strength under axial loading

f_b – design compressive strength of concrete (taken from Table 15 of PBAB 87)

MB – concrete grade, from which the nominal compressive strength of concrete (f^{bk}) in MPa is derived, based on the characteristic cube strength at an age greater than 28 days.

$$E_b = 9.25 \cdot \sqrt[3]{f_{bk} + 10} \quad (2)$$

Eb – mean value of the modulus of elasticity of concrete

f_{zs} – flexural tensile strength (taken from Table 2 of SRPS U.E3.020)

According to Article 75 of PBAB 87, the design of reinforced concrete elements is based on ultimate and serviceability limit state verification. For concrete pavement structures, particularly airport slabs, design practice is predominantly governed by serviceability limit state criteria, where—both in PBAB 87 and in EN 206 / Eurocode 2—the calculations are performed without applying partial safety factors. Differences in design outcomes mainly arise from the different definitions of characteristic flexural tensile strength of concrete and the associated acceptance criteria.

3.2 PROPERTIES OF CONCRETE ACCORDING TO EN 206 AND EC 2

EN 206:2021 and Eurocode 2 define concrete properties through a system of characteristic and mean strength values. For the purposes of slabs-on-ground-particularly external manipulation and traffic-bearing surfaces—the most important parameters are:

C – concrete strength class, cylinder/cube.

f_{ck} – characteristic compressive strength of a concrete cylinder at 28 days (taken from Table 3.1 of SRPS EN 1992-1-1:2015)

$f_{ck,cube}$ – characteristic compressive strength of a concrete cube at 28 days (taken from Table 3.1 of SRPS EN 1992-1-1:2015)

f_{cm} – mean compressive strength of concrete cylinder

$$f_{cm} = f_{ck} + 8\ \text{MPa} \quad (3)$$

f_{ctm} – mean value of concrete tensile strength under axial loading

$$f_{ctm} = 0.30 \cdot f_{ck}^{(2/3)} \quad za \le C50/60 \quad (4)$$

$$f_{ctm} = 2.12 \cdot \ln(1 + (f_{cm}/10)) \quad za > C50/60 \quad (5)$$

E_{cm} – secant modulus of elasticity of concrete

$$E_{cm} = 22 \cdot [f_{cm}/10]^{0.3} \quad (6)$$

$f_{ctm,fl}$ – characteristic value of concrete flexural tensile strength

$$f_{ctm,fl} = (1.6 - h/1000) \cdot f_{ctm} \quad (7)$$

f_{cd} – design compressive strength of concrete

$$f_{cd} = \alpha_{cc} \cdot f_{ck}/\gamma_c \quad (8)$$

α_{cc} - coefficient accounting for long-term effects and unfavorable load application conditions

γ_c - partial safety factor for concrete

Thus, EN 206/EC 2 introduces a strictly defined statistical basis for characteristic values, which directly influences safety factors and design stress values.

3.3 COMPARISON OF CONCRETE PROPERTIES ACCORDING TO PBAB / SRPS U.E3.020 AND EN 206 / EC2

Table 1 presents the differences between the two systems of concrete properties used in the design of slabs-on-ground.

Table 1. Comparison of concrete properties according to PBAB 87 / SRPS U.E3.020 and EN 206 / EC2 (example: MB35 vs. C30/37)

Concrete parameter	PBAB 87/ SRPS U.E3.020	EN 206/ EC 2	Note
f_{bk} / $f_{ck,cube}$	35 MPa	37 MPa	partially compatible in compression
f_{bzm} / f_{ctm}	2.67 MPa	2.90 MPa	approximate values
f_{zs} / $f_{ctm,fl}$	4.5 MPa	4.0 MPa	always lower per EC2
E_b / E_{cm}	32.9 GPa	32.8 GPa	similar values
f_b / f_{cd}	23 MPa	17 MPa	always lower per EC2

Differences in the definition of characteristic tensile-strength values lead to differences in allowable and ultimate flexural stresses and, consequently, in determining the minimum

required slab thickness. PBAB 87 uses higher flexural tensile strength values, while EN 206 / EC2 introduces consistently defined characteristic values and safety concepts. In practice, this means that under the same subgrade conditions, the same wheel load, and the same load position, the design thickness may differ depending on which material model is applied. This difference will be quantitatively analysed in the following section.

4. NUMERICAL ANALYSIS OF THE INFLUENCE OF THE MATERIAL MODEL ON SLAB DESIGN

To assess the influence of the concrete material model on the results of Westergaard's slab-on-ground analysis, a comparative study was carried out for concrete slabs with thicknesses of 18, 20, 22, and 24 cm, designed using concrete class MB35 according to PBAB 87 and C30/37 concrete according to EN 206 and EC 2. The analysis includes calculation of subgrade reaction modulus, Westergaard's radius of relative stiffness, characteristic flexural stresses in the edge loading position, and comparison with the concrete strength limits according to both models. It is performed through the following steps:

- determination of input parameters and material properties;
- calculation of the subgrade reaction modulus *k*;
- determination of Westergaard's radius of relative stiffness *l*;
- calculation of the equivalent contact radius *r*;
- calculation of flexural stresses for characteristic load positions;
- comparison with the ultimate concrete strengths according to PBAB and EC2;
- presentation of results in tabular form.

4.1 INPUT DATA FOR THE ANALYSIS

Descriptions of the parameters are given below.

- Load:
- Tractor unit with semi-trailer
- Design axle load: 115 kN
- Number of wheels per axle: n = 4
- Tire pressure: p = 650 kPa
- Tandem wheel spacing: Sd = 0.373 m
- Radius of the equivalent circular contact area: r = 0.216 m
- Load per dual wheel: $Q_k/2$ = 57.5 kN

- Subgrade:

The subgrade reaction modulus *k* is determined using Vesić's method:

$$k = \frac{0.65 \cdot E_s}{B \cdot \left(1 - \nu_s^{\,2}\right)} \cdot \sqrt[12]{\frac{E_s \cdot B^4}{E_c I}} \tag{9}$$

where:

- E_s – modulus of elasticity of the soil/subgrade
- B – characteristic slab width – 1.0 m
- ν_s – Poisson's ratio of the soil/subgrade
- E_c – modulus of elasticity of concrete

- Concrete:

The following models are compared:

- MB35 (PBAB 87)
- C30/37 (EN 206 / EC2)

Relevant values from Table 1 are introduced into the calculation for each slab thickness.

4.2 WESTERGAARD'S RADIUS OF RELATIVE STIFFNESS AND FLEXURAL STRESSES

Westergaard's radius of relative stiffness is calculated as:

$$l = \left(\frac{E_c \cdot h^3}{12k \cdot \left(1 - \nu_c^{\,2}\right)} \right)^{1/4} \tag{10}$$

with Poisson's ratio of concrete ν_c = 0.15.

The radius of the equivalent wheel-contact area depends on the load and the tire–slab contact characteristics, while the ratio ℓ/a enters directly into Westergaard's expressions for stresses.

For the edge loading case (critical for a slab without dowels), the flexural stress is calculated using:

$$\sigma_e = \frac{3 \cdot (1 + \nu_c) \cdot PE}{\pi \cdot (3 + \nu_c) \cdot h^2} \cdot \left[\ln\left(\frac{E_c \cdot h^3}{100\,k \cdot a^4} \right) + 3.84 - \left(\frac{4 \cdot \nu_c}{3} \right) + \frac{(1 + 2 \cdot \nu_c) \cdot a}{2 \cdot l} \right] \tag{11}$$

This stress is compared, for each slab thickness, with the ultimate concrete strengths according to the two models:

- PBAB 87: flexural tensile strength, f_{zs}

- EC2: characteristic value of flexural tensile strength, $f_{ctm,fl}$

4.4 COMPARATIVE ANALYSIS

Table 2 presents the key parameters and calculation results for all analysed slab thicknesses and both material models. The table includes the subgrade reaction modulus, Westergaard's radius of relative stiffness, calculated flexural stresses σe, ultimate concrete strength values, and the fulfilment of criteria. The results indicate consistent differences between the two approaches:

- the concrete modulus of elasticity has a very small influence on the subgrade reaction coefficient and therefore on Westergaard's radius of relative stiffness;
- differences in ℓ further affect the logarithmic component of Westergaard's equations and thus the magnitude of the edge stress σ_e;
- the flexural and tensile strengths of concrete define the ultimate stress values, whereby PBAB uses higher limit values of flexural tensile strength, while EC2 defines lower characteristic flexural tensile strength values $f_{ctm,fl}$ dependent on slab thickness;
- the combined effect of these differences leads to different required slab thicknesses depending on the selected concrete material model.

Table 2. Comparative overview of key parameters and calculation results according to PBAB and EN 206/EC2

Slab thickness h (cm)	Concrete model	Edge stress σ_e (MPa)	Ultimate stress value (MPa)
18	PBAB	4.623	4.500
18	EC2	4.621	4.113
20	PBAB	3.910	4.500
20	EC2	3.909	4.055
22	PBAB	3.555	4.500
22	EC2	3.354	3.997
24	PBAB	2.915	4.500
24	EC2	2.914	3.939

5. DISCUSSION

The results of the numerical analysis show that the stress states in the concrete slab are practically identical regardless of whether material parameters according to PBAB 87 or EN 206/EC2 are used. Differences in the edge stress σe amount to only 0.002–0.2 MPa, depending on slab thickness and concrete grade/class, which represents a negligible deviation in the context of the overall accuracy of Westergaard's model. This outcome is a consequence of the fact that the elastic moduli E in both approaches have very similar values, and that the calculation of the subgrade reaction modulus and Westergaard's radius of relative stiffness yields almost identical results.

Although the mechanical part of the calculation produces virtually the same response, a significant difference appears in the concrete strength criterion. The PBAB methodology is based on a flexural strength $f_{zs} \approx 4.50$ MPa, which is taken as constant and independent of slab thickness. In contrast, EN 206/EC2 uses the characteristic value of concrete flexural tensile strength $f_{ctm,fl}$, which is lower than f_{zs}. Therefore, the difference in ultimate stress values is much larger than the difference in calculated stresses. For all analysed slab thicknesses, PBAB 87 allows higher stresses (4.50 MPa), while the characteristic values according to EC2 range from 4.11 to 3.94 MPa, resulting in lower available capacity in the EC2 approach.

Despite the fact that stresses are practically equal, the EC2 strength criterion leads to a greater required slab thickness compared to PBAB. This means that the difference in design outcomes originates almost exclusively from the different philosophies of defining concrete ultimate strengths, rather than from any difference in the mechanical model of a slab on an elastic foundation.

This finding is particularly important in the context of standard harmonisation, as it indicates that the transition from the PBAB model to the EN 206/EC2 framework does not change the stress state in the concrete slab; instead, it introduces a stricter and statistically defined serviceability-and subsequently ultimate-strength criterion. This ensures consistency with contemporary European standards, but in practice results in the need for greater slab thicknesses, especially for external manipulation and traffic-bearing surfaces exposed to cyclic and climatic effects.

6. CONCLUSION

This paper presents an analysis of the differences in the design of concrete slabs-on-ground arising from the application of two different concrete material models: PBAB 87 (MB35) and EN 206/EC2 (C30/37). The objective was to quantify the influence of differences in defining the mechanical properties of concrete on the results of Westergaard's calculation and on the serviceability and ultimate limit state criteria of the structure.

The results show that the differences in calculated flexural stresses between the two approaches are negligible. The subgrade reaction modulus and Westergaard's radius of relative stiffness remain practically unchanged when switching from PBAB 87 to EC2, leading to almost identical stress values in the critical load positions. This indicates that the choice of material design model does not significantly influence the mechanical response of the slab within the framework of Westergaard's theory.

However, the key difference arises in the strength criterion. PBAB 87 uses the flexural tensile strength f_{zs} as the allowable value, which is relatively high and independent of statistical parameters. In contrast, EN 206/EC2 defines concrete tensile strength through characteristic values. As a result, even with identical stresses, the available structural capacity according to EC2 is nominally lower.

Consequently, for the same loading and subgrade conditions, the PBAB 87 methodology yields thinner slabs compared to the EC2 approach. For external manipulation and traffic-bearing surfaces, where cyclic loading, frost, and chlorides are dominant influences, the application of EC2 provides a more conservative and reliable result, requiring greater slab thickness relative to our practice.

The findings indicate that the transition to European regulation does not change the fundamental mechanics of slab-on-ground design but introduces a modern and statistically based strength criterion that ensures a higher level of structural safety. In this sense, the harmonization of design standards for concrete pavements and industrial slabs with EN 206/EC2 represents a logical step toward unifying practice and increasing the reliability of engineering solutions.

It is worth noting that the draft of the second-generation Eurocode 2 does not introduce specific design models for concrete slabs-on-ground, nor does it modify the definition of characteristic or design tensile strengths that would be relevant for such structures. Accordingly, the differences identified between the PBAB 87 and EN 206/EC2 approaches, as well as the conclusions drawn in this paper, remain fully applicable in the context of the forthcoming EC2:2025 revision.

REFERENCES

[1] American Concrete Institute (2010). ACI 360R-10: Guide to Design of Slabs-on-Ground. ACI Committee 360, Farmington Hills, Michigan.

[2] Bamforth, P., Chisholm, D., Gibbs, J., Harrison, T. (2008), Properties of Concrete for Use in Eurocode 2, The Concrete Centre, UK.

[3] CEN (2004), EN 1992-1-1: Eurocode 2 – Design of Concrete Structures – Part 1-1: General Rules and Rules for Buildings, European Committee for Standardization.

[4] CEN (2021), EN 206:2013+A2:2021 – Concrete: Specification, Performance, Production and Conformity, European Committee for Standardization.

[5] Cvetanović, A. i Banić, B. (2007). Kolovozne konstrukcije. Akademska misao, Beograd.

[6] Institut za standardizaciju Srbije (1987), SRPS U.E3.020 – Tehnički uslovi za izradu cementnobetonskog kolovoza, ISS.

[7] Institut za standardizaciju Srbije (1994), SRPS U.C4.014 – Dimenzionisanje novih cementnobetonskih kolovoznih konstrukcija, ISS.

[8] Institut za standardizaciju Srbije (2011). SRPS EN 13670:2011 – Izvođenje betonskih konstrukcija. Beograd.

[9] Matić, M. (2018). Metodološke osnove za planiranje i projektovanje STOL aerodroma za mali saobraćaj – primer aerodroma "Paraćin"-Davidovac. Master rad, Fakultet tehničkih nauka, Univerzitet u Novom Sadu, Novi Sad.

[10] Ministarstvo građevinarstva, saobraćaja i infrastrukture (2023/2024), Pravilnik o tehničkim zahtevima za beton, „Službeni glasnik RS", br. 48/2023 и 78/2024.

[11] Portland Cement Association (2001). Concrete Floors on Ground. PCA, Skokie, Illinois.

[12] Savezni zavod za standardizaciju (1987), BAB 87 – Pravilnik o tehničkim normativima za beton i armirani beton, Službeni list SFRJ.

[13] The Concrete Society (2003), TR34 – Concrete Industrial Ground Floors: A Guide to Design and Construction, Technical Report No. 34, 3rd Edition, UK.

[14] Transport Research Laboratory (1999), Concrete Pavement Design Guidance Notes, TRL Report, UK.

[15] Uzelac, Đ. (2015), Kolovozne konstrukcije, FTN Izdavaštvo, Novi Sad.

Riste Ristov
MSc, Teaching Assistant
Ss. Cyril and Methodius University in Skopje
Faculty of Civil Engineering Skopje
North Macedonia
ristov@gf.ukim.edu.mk
0000-0002-4996-0382

IDENTIFICATION OF KEY RISK FACTORS FOR TRAFFIC ACCIDENTS USING MACHINE LEARNING

Received: 27.11.2025
Accepted: 05.02.2026
Published: 06.02.2026

DOI: 10.55302/SJCE2514223r

Road safety represents a significant challenge for the transport sector due to the severe consequences of traffic accidents and the need for timely identification of factors that increase risk. This study aims to quantify the influence of selected parameters on the weighted accident index and to establish a foundation for predictive models capable of identifying high-risk road sections. The analysis covers 161 sections of the national road network in the Republic of North Macedonia, with a total length of approximately 1,300 km, and includes 23 parameters. The assessment was performed using machine learning techniques, with model evaluation conducted on an 80/20 train–test split. The results reveal that road characteristics and traffic volume (AADT) exert the greatest influence on accident risk, whereas environmental factors have minimal impact. This approach enables more efficient planning of interventions and contributes to the overall improvement of road safety.

Keywords: accidents, machine learning, roads, safety, weighted index

1. INTRODUCTION

Traffic accidents represent one of the most serious global public-safety challenges, particularly among younger populations. According to the World Health Organization [1], road traffic injuries are the leading cause of death for individuals aged 5 to 29 years, claiming more than 1.19 million lives annually. Although developed countries have achieved considerable progress through systematic measures and infrastructure improvements, the average fatality rate in the European Union remains 45.5 deaths per million inhabitants [2].

In North Macedonia the situation is particularly concerning, with a rate of 69.5 fatalities per

Scientific Journal of Civil Engineering (SJCE)
© 2025 by Faculty of Civil Engineering, SCMU - Skopje is licensed under CC BY-SA 4.0

million inhabitants [3], significantly above the European average. These figures underscore the urgent need for a proactive approach to road safety that does not rely solely on historical accident records but enables the identification and prediction of high-risk segments, allowing timely preventive interventions.

Modern analytical tools, such as machine learning and geospatial analysis, facilitate the detection of high-risk sections even before accidents occur. This proactive strategy substantially enhances the ability to plan targeted safety measures and manage risk across the road network more effectively.

The objective of this research is to determine the most influential factors affecting the weighted accident index (Wi) and to establish a foundation for predictive models that will support more efficient prioritization of interventions and national-level risk management.

2. LITERATURE REVIEW

The application of machine learning in the analysis of traffic accident risk factors has advanced significantly in recent years.

Wang [4] analyzed rural road accidents using Random Forest and SHAP values and identified road geometry and pavement condition (horizontal curves, longitudinal gradients, friction coefficient, sight distance, and signage) as dominant factors, parameters that strongly overlap with those in the present study.

Jiang [5] combined urban and national databases and confirmed that weather conditions and lighting have noticeable but clearly weaker influence than road characteristics and traffic volume (AADT).

Çelik [6] compared multiple techniques on large accident datasets and demonstrated that tree-based methods, including XGBoost, provide high accuracy and efficiency, supporting the models selected for this research.

These studies are fully consistent with the current findings: road geometry, pavement condition, and traffic volume are the primary risk drivers, while environmental factors play only a secondary role.

3. DATA AND MATERIALS

3.1 GENERAL INFORMATION ON THE ROAD NETWORK

The road network of the Republic of North Macedonia has a total length of 14,475 km and is classified into national, regional and local roads [7]. The national road network has a length of 897 km and represents a key segment of both national and trans-European transport infrastructure [8]. It comprises motorways, expressways, and two-lane roads that provide the main traffic connections within the country and with neighboring states.

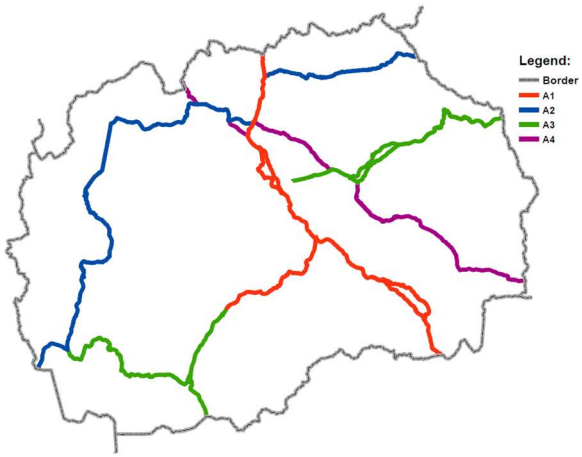


Figure 1. Overview map of Category A roads

The present research focuses on the national roads A1, A2, A3, and A4, which differ in technical characteristics and geometric elements. Although the official length of the national road network is 897 km, the analysis covers approximately 1,300 km due to the separate treatment of each carriageway on roads with divided lanes (motorways).

3.2 DESCRIPTION AND PROCESSING OF THE DATA

The data were processed using GIS tools, statistical techniques, and machine-learning methods, enabling the identification of spatial and temporal trends.

- Road characteristics. This category includes various geometric and functional parameters such as speed limits, horizontal curvature, curve radii, longitudinal gradients, and elevation. Additionally, lateral forces in curves, stopping sight distance, pavement evenness, rut depth, surface friction coefficient, and pavement condition index are analyzed. Data on the density of junctions, bridges, and viaducts, as well as

the condition of vertical and horizontal signage, are also incorporated [9][10].

- Traffic characteristics. Traffic intensity is expressed through annual average daily traffic (AADT), based on fixed and mobile automatic counts. This parameter provides insight into the influence of traffic volume on risk [11].

- Environmental characteristics. Climatic factors are represented by average and extreme annual values of precipitation and temperature, collected over a ten-year period from relevant meteorological stations. The data were processed using geospatial methods to achieve high resolution at the level of individual road sections [12].

- Accident data. The frequency and spatial distribution of traffic accidents were analyzed using a weighted accident index that takes into account both the number and severity of accidents. The index is based on a weighted scoring system according to injury severity and is normalized by the length of each road section. This index serves as the primary indicator for assessing and comparing the safety performance of different sections of the road network [13].

4. METHODOLOGY

The methodology investigates the factors influencing traffic accident risk using three machine-learning models: Bagging Regressor, CatBoost Regressor, and LightGBM Regressor. These models were selected to quantify the influence of 23 parameters (road geometry, traffic conditions, and environmental factors) on the weighted accident index (Wi).

The dataset comprising 161 road sections was divided into training 80% and test 20% subsets using stratified random sampling to preserve the distribution of the target variable. Model performance was evaluated on the test set using the coefficient of determination (R^2), mean absolute error (MAE), and root mean square error (RMSE).

The three models provide complementary strengths: Bagging Regressor reduces variance and ensures robustness, CatBoost Regressor efficiently handles categorical features and prevents overfitting, while LightGBM Regressor offers fast training and high accuracy through gradient boosting. Their combination yields stable and highly interpretable rankings of parameter importance.

5. RESULTS

5.1 BAGGING REGRESSOR

Bagging Regressor relies on the combination of multiple independent models to improve the stability and accuracy of predictions through the averaging of their outputs. Instead of depending on a single model, the method generates different subsets of the original dataset, each used to train a separate base learner, typically a decision tree. By aggregating their predictions, this technique produces more balanced and robust estimates, particularly when dealing with variable or complex data [14].

In the present study, the method was employed to predict the weighted accident index (Wi). The model consists of 500 decision trees, each trained on a different bootstrap sample, with their aggregation ensuring more uniform estimates and variance reduction.

The general prediction formula can be expressed as follows:

$$Y = (1/T)\sum(t = 1)^{T} Y_t \quad (1)$$

The final prediction Y is the average of all individual tree predictions, where Y_t is the prediction of each individual model and T is the total number of models.

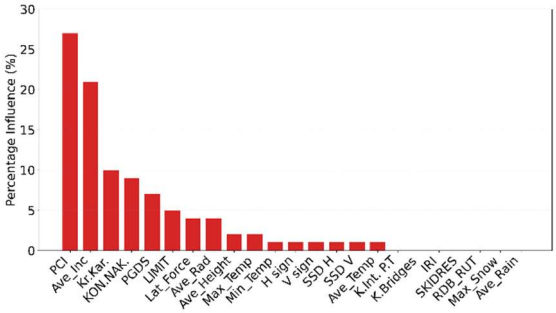


Figure 2. Percentage influence (Bagging Regressor)

As shown in the figure 2, the pavement condition index (PCI) and average longitudinal gradient (Ave_Inc) exert the strongest influence, traffic-related parameters exhibit moderate influence, while parameters associated with weather conditions have minimal impact.

The Bagging Regressor demonstrates solid predictive performance with R^2 = 0.522, MAE =

2.89, and RMSE = 3.78 on the test set, reflecting sensitivity to larger deviations.

5.2 LIGHTGBM REGRESSOR

With this technique, trees are added incrementally, growing along the most beneficial leaf (leaf-wise), and histogram-based thresholds are used for each feature to accelerate split selection [15]. This approach is well-suited to tabular data comprising section-wise indicators with the weighted accident index (Wi) as the target. The model deepens the leaf that yields the greatest local improvement, while feature histograms provide a limited set of candidate thresholds. This enables rapid model enhancement with moderate complexity and easily interpretable leaf rules.

In its simplest form, the update follows the gradient boosting scheme:

$$F_m(x) = F_{m-1}(x) + \gamma \cdot h_m(x) \quad (2)$$

Where $F_m(x)$ is the new predictive model after the m-th iteration, $F_{m-1}(x)$ is the previous model, $h_m(x)$ is the weak learner that corrects the previous errors and γ is the learning rate that controls the contribution of the new model. For selecting a split s (potential node split), the gain metric is used:

$$(s) = 0.5 * \left(G_L(s)^2/(H_L(s) + \lambda) + G_R(s)^2/ (H_R(s) + \lambda) - G(s)^2/(H(s) + \lambda)\right) - c \quad (3)$$

Where G and H are the sums of the first and second derivatives of the loss at the node and sides, λ is the L2 regularisation on complexity and γ is the fixed penalty for gain per split.

In this research, the method was applied to predict the weighted accident index (Wi). The model was optimised with 400 iterations, learning_rate ≈ 0.005, num_leaves = 7, and additional regularisation and subsampling parameters.

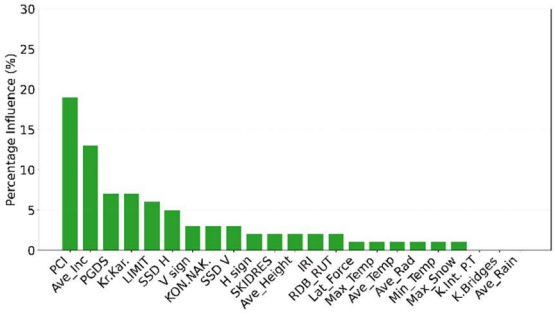


Figure 3. Percentage influence (LGBM)

As shown in the figure 3, road-related parameters (PCI, Ave_Inc, Kr.Kar.) and traffic-related parameters (PGDS, LIMIT) are clearly the most influential, while environmental parameters (precipitation, snow, temperature, elevation) have minimal influence.

The LightGBM Regressor achieved $R^2 = 0.514$, MAE = 2.94, and RMSE = 3.85 on the test set, confirming stable and accurate predictions.

5.3 CATBOOST REGRESSOR

CatBoost is a method that builds small symmetric trees and combines them into a stronger model. When categorical features are present, it encodes them using ordered target statistics, ensuring that each record uses information only from preceding rows and preventing information leakage from training to test data. It is particularly suitable for tabular data containing a mixture of numerical and categorical variables, requires no prior standardisation, and delivers stable estimates with simple and interpretable rules [16]. The model achieves progressive error reduction, with categorical features encoded in order (ordered encoding) without using information from future rows.

In its simplest form, the update follows the gradient boosting scheme:

$$F_m(x) = F_{m-1}(x) + \gamma \cdot h_m(x) \quad (4)$$

Where $F_m(x)$ is the new predictive model after the m-th iteration, $F_{m-1}(x)$ is the previous model, $h_m(x)$ is the weak learner that corrects the previous errors and γ is the learning rate. Categorical variables are transformed into numerical values using ordered statistics:

$$\mathrm{enc}(\mathrm{cat_i}) = \left(\Sigma_{j<i} y_j + a * \mathrm{prior}\right)/(n_{<i} + a) \quad (5)$$

Where $\mathrm{enc}(\mathrm{cat_i})$ is the encoded value for the category in the current row i, j < i – previous rows and prior is the initial value for stabilisation, a is the smoothing coefficient.

This ordered encoding between training and test sets is fully consistent with the 80/20 split and eliminates information overlap.

In this research, the method was applied to predict the weighted accident index (Wi). The model was configured with 1000 iterations, learning_rate = 0.05, and depth = 6.

As clearly visible from the figure 4, the dominant influence on the weighted accident index is exerted by road and traffic characteristics (PCI, Ave_Inc, PGDS, Kr.Kar., KON.NAK., LIMIT),

whereas the influence of environmental factors (precipitation, snow, temperature, and elevation) is negligible.

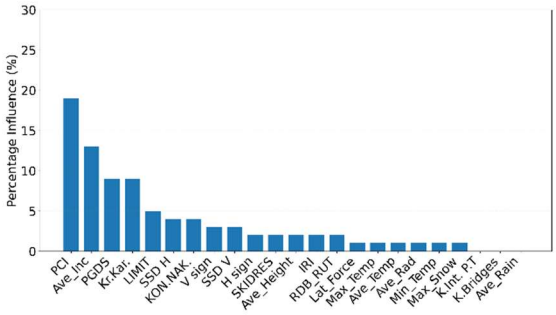


Figure 4. Percentage influence (CatBoost)

On the test set, CatBoost Regressor obtained R^2 = 0.520, MAE = 2.91, and RMSE = 3.81, confirming robust and predictive reliability.

5.4 AVERAGING AND NORMALISATION OF RESULTS FROM THE THREE METHODS

This section presents the combined results obtained from the three applied machine-learning models used to evaluate the influence of various factors on the weighted accident index (Wi).

To ensure a balanced evaluation, the importance of the parameters was averaged using weights proportional to the accuracy (R^2) of each model on the test subset (80/20):

- Bagging Regressor (33.7 %) – R^2 = 0.522
- CatBoost Regressor (33.5 %) – R^2 = 0.520
- LightGBM Regressor (32.8 %) – R^2 = 0.514

Based on these weights, the percentage influence values from the three methods were normalised so that the total sum across all parameters equals 100 %. This approach provides a more objective and comparable assessment of the significance of the factors.

Table 1. Percentage influence of parameters on the weighted accident index (Wi)

No.	Abbr.	BR (%)	CB (%)	LGBM (%)	Res. (%)
1	PCI	27.0	19.0	19.0	**22.8**
2	Ave_Inc	21.0	13.0	13.0	**16.6**
3	Kr.Kar.	10.0	9.0	7.0	**9.0**
4	PGDS	7.0	9.0	7.0	**7.8**
5	KON.NAK.	9.0	4.0	3.0	**6.1**
6	LIMIT	5.0	5.0	6.0	**5.3**
7	RDB_RUT	0.0	2.0	2.0	**1.2**
8	K.Int. P.T	0.0	0.0	0.0	**0.0**
9	IRI	0.0	2.0	2.0	**1.2**
10	SSD H	1.0	4.0	5.0	**3.1**
11	K.Bridges	0.0	0.0	0.0	**0.0**
12	V sign	1.0	3.0	3.0	**2.2**
13	SSD V	1.0	3.0	3.0	**2.2**
14	Lat_Force	4.0	1.0	1.0	**2.3**
15	Ave_Temp	1.0	1.0	1.0	**1.0**
16	Ave_Rad	4.0	1.0	1.0	**2.3**
17	Ave_Rain	0.0	0.0	0.0	**0.0**
18	Max_Snow	0.0	1.0	1.0	**0.6**
19	Min_Temp	1.0	1.0	1.0	**1.0**
20	Ave_Height	2.0	2.0	2.0	**2.0**
21	SKIDRES	0.0	2.0	2.0	**1.2**
22	Max_Temp	2.0	1.0	1.0	**1.5**
23	H sign	1.0	2.0	2.0	**1.6**

The resultant values, shown in Figure 5, indicate that the most influential factors are clearly the pavement condition index (PCI), the average longitudinal gradient (Ave_Inc), and the horizontal curvature characteristic (Kr.Kar.). Conversely, the lowest influence is exhibited by skid resistance (SKIDRES), maximum annual temperatures (Max_Temp), and horizontal signage (H sign).

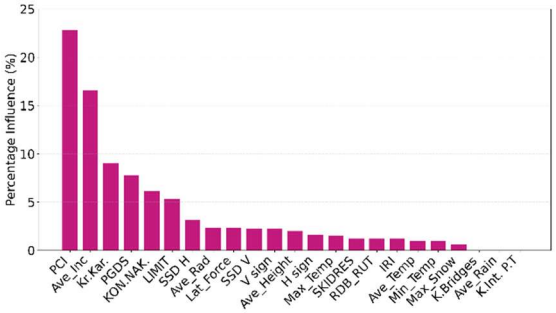


Figure 5. Normalised influence of parameters

The combined evaluation confirms the priority of measures aimed at pavement maintenance, management of longitudinal gradients, and improvement of horizontal alignment geometry. Factors with the lowest influence are useful as supplementary indicators and should be monitored contextually, without decisive impact on ranking.

6. DISCUSSION

The analysis reveals that the greatest influence on the weighted accident index is exerted by the geometric and structural characteristics of the road, particularly the pavement condition index (PCI), average longitudinal gradient (Ave_Inc), and horizontal curvature characteristic (Kr.Kar.). Together, these parameters account for 51.4 % of the total influence, highlighting their critical role in determining road safety. Parameters related to operational conditions exhibit moderate influence, whereas environmental factors contribute negligibly.

In a comparative context, the three models demonstrate a high degree of consistency.

Bagging Regressor provides the highest accuracy and robustness, CatBoost Regressor excels in interpretability and effective handling of categorical data, while LightGBM Regressor offers the fastest training with virtually identical rankings and only minimal deviations. This consistent ordering of the leading factors across all three models strongly reinforces the conclusions regarding priorities and supports the implementation of measures focused on improving pavement condition and managing longitudinal gradients and horizontal curves.

7. CONCLUSION

In summary, the results indicate that traffic-accident risk is primarily determined by pavement condition and road geometry. Indicators related to surface damage, longitudinal gradient, and horizontal curvature clearly dominate over all other variable groups. Parameters linked to operational conditions have a moderate contribution, while environmental factors prove negligible in the analyzed dataset.

The combination of three decision-tree-based machine-learning models (Bagging Regressor, CatBoost Regressor, and LightGBM Regressor) together with evaluation on an 80/20 train–test split provides a stable, robust, and highly interpretable assessment of the parameters, yielding consistent ranking of the key factors. These findings support the identification of high-risk sections and lay the foundation for predictive tools that will facilitate the planning and prioritization of road-safety interventions.

Future research should focus on expanding the database and incorporating additional parameters (e.g. share of heavy vehicles, actual speeds, lane and shoulder widths), as well as introducing finer temporal resolution and external validation across different road categories. Such steps would strengthen the general applicability and increase the practical value of the results.

REFERENCES

[1] World Health Organization. (2024). Road traffic injuries.
Available at: https://www.who.int/news-room/fact-sheets/detail/road-traffic-injuries (accessed March 2025).

[2] European Commission. (2023). Road Safety Statistics 2023. Available at: https://road-safety.transport.ec.europa.eu/european-road-safety-observatory_en (accessed March 2025).

[3] State Statistical Office of the Republic of North Macedonia. (2025).
MakStat – Statistical database. Available at: https://makstat.stat.gov.mk/PXWeb/pxweb/mk/ (accessed March 2025).

[4] Wang, Y., Zhang, Y., Wu, J., & Xu, C. (2023). Analyzing the Risk Factors of Traffic Accident Severity Using Machine Learning and Association Rules. International Journal of Environmental Research and Public Health, 20(1), 345. https://doi.org/10.3390/ijerph20010345

[5] Jiang, Y., Li, S., Zhao, Z., & Chen, H. (2024). Machine Learning-Based Prediction Analysis of Potential Factors Influencing Traffic Accident Severity. Sustainability, 16(2), 1125. https://doi.org/10.3390/su16021125

[6] Çelik, E., & Sevli, D. (2022). Predicting Road Traffic Accident Severity Using Machine Learning Techniques. Applied Sciences, 12(15), 7485. https://doi.org/10.3390/app12157485

[7] Public Enterprise for State Roads. Web-GIS platform for spatial analysis and visualisation. Available at: http://62.77.137.99/pesr/webgis/#/map (accessed March 2025).

[8] Ministry of Local Self-Government. (2021). Programme for Development of the Planning Regions for the period 2021–2026. Government of the Republic of North Macedonia, Skopje.

[9] Doncheva, R., Ognjenovic, S. (2024). Road Design. Ss. Cyril and Methodius University – Faculty of Civil Engineering, Skopje. ISBN: 978-608-4510-60-4.

[10] Tobias, P., de León Izeppi, E., Flintsch, G., Katicha, S., McCarthy, R. (2023). Pavement Friction for Road Safety: Primer on Friction Measurement and Management Methods. Federal Highway Administration (FHWA), Report No. FHWA-SA-23-007.

[11] Public Enterprise for State Roads. Web-GIS platform for spatial analysis and visualisation. Available at: http://tdps.roads.org.mk/ (accessed March 2025).

[12] Gjeshovska, V., Taseski, G., Ilioski, B. (2024). Intense precipitation in the Republic of North Macedonia. Ss. Cyril and Methodius University – Faculty of Civil Engineering, Skopje. ISBN: 978-608-4510-56-7.

[13] Government of the Republic of North Macedonia, Ministry of Transport, Project Unit. (2024). Black Spot Management Handbook (BSM). Skopje, July 2024.

[14] Patil, P., Du, J.-H., Kuchibhotla, A. K. (2022). Bagging in overparameterized learning: Risk characterization and risk monotonization. arXiv preprint,arXiv:2210.11445.https://doi.org/10.48550/arXiv.2210.11445

[15] Ke, G., Meng, Q., Finley, T. et al. (2017). LightGBM: A Highly Efficient Gradient Boosting Decision Tree. Advances in Neural Information Processing Systems, 30. Available at: https://proceedings.neurips.cc/paper_files/paper/2017/file/6449f44a102fde848669bdd9eb6b76fa-Paper.pdf

[16] Prokhorenkova, L., Gusev, G., Vorobev, A., Dorogush, A. V., & Gulin, A. (2018). CatBoost: unbiased boosting with categorical features. Advances in Neural Information Processing Systems,31.https://doi.org/10.48550/arXiv.1706.09516

SELECT A PROFESSION

CREATIVE	SOPHISTICATED	RECOGNIZED	RESPONSIBLE
ENDURING	UP-TO-DATE	WORLWIDE	IMPORTANT

WWW.GF.UKIM.EDU.MK

OUR FACULTY CAN GIVE YOU

IMPULSE !	SCHOLARSHIPS FOR THE BEST	ASSURANCE !	COORPERATION WITH INDUSTRY AND INTERNATIONAL UNIVERSITIES
SIMPLE ENROLLMENT	MOTIVATION !	100% EMPLOYMENT AND INTERNATIONALLY RECOGNIZED DIPLOMA	SUPPORT !

WWW.GF.UKIM.EDU.MK

Valentina Zileska Pancovska
Professor, PhD
Ss. Cyril and Methodius University
Faculty of Civil Engineering Skopje
North Macedonia
valentinazp@gf.ukim.edu.mk
0000-0001-7620-4040

Todorka Samardzioska
Professor, PhD
Ss. Cyril and Methodius University
Faculty of Civil Engineering Skopje
North Macedonia
0000-0001-8992-2279

Sead Abazi
Assistant Professor, PhD
Ss. Cyril and Methodius University
Faculty of Civil Engineering Skopje
North Macedonia
0000-0001-8263-600X

Emil Ajdinoski
Civil Engineer, MSc
TD Constructor DOOEL – Struga
North Macedonia

Scientific Journal of Civil Engineering (SJCE)
© 2025 by Faculty of Civil Engineering, SCMU - Skopje is licensed under CC BY-SA 4.0

COST STRUCTURE FOR RESIDENTIAL BUILDINGS WITH REINFORCED CONCRETE STRUCTURAL SYSTEM

Received: 25.11.2025
Accepted: 13.02.2026
Published: 05.03.2026

DOI: 10.55302/SJCE2514231z

Determining the participation of each type of works in the total construction costs for the building is a useful issue, particularly in the early stage of the project. Therefore, data has been collected for fifteen residential buildings built in Macedonia. Buildings have reinforced-concrete structures, one underground level and four to seven levels above the ground. The participation of each type of works in the total construction costs for each building was calculated. Their average participation is: earth works 3,02 %, concrete and reinforced-concrete works – 41,55 %, masonry works – 10,84 %, roofing works – 2,44 %, plastering – 14,67 %, painting – 0,76 %, floor works – 12,95 %, insulation works – 4,22 %, doors and windows – 9,55 %. Although the values presented are approximate, they can be used to roughly predict costs of each type of work for residential buildings with reinforced concrete structure.

Keywords: costs, cost structure, construction works, residential buildings, reinforced-concrete structural system.

1. INTRODUCTION

The accuracy in the estimation of construction costs, as well as the project budget; always have an influence on the building construction and the project participants' work [1]. Therefore, knowing the building cost structure is a useful for all project participants, although its determination is a complex procedure. Hence, it is an imperative to determine the participation of each type of works in the total construction costs for the building with satisfactory accuracy [2].

Globally, building costs are determined by many factors whose influence depends on a set

of circumstances, such as conditions of the building location and its' surrounding, the impact on the environment, market conditions, the investor's wishes and needs (including the luxury of the building), the pricing methodology applied by each of the participants in the construction project, etc. [3-5]. Furthermore, costs are influenced by the type of contract signed between the project participants, the sustainability rating of the building, the references and reputation of the project participant, the method used for cost forecast, the expertise and experience of the personnel who calculate the costs, software application etc. [6-10].

The building costs are also impacted by the complexity and duration of the construction process, which usually lasts for months or years. During that period, usually there are changes in the costs of materials, human resources and energy, which directly affect the construction costs [11, 12]. Furthermore, there are other circumstances related to the total costs, such as: influences on the cash flow; financial activities faced by project participants; influences on profit percentage; delay of construction; delay of incomes; interruption of the construction process; supply of materials, machines, equipment and other resources; usage of recycled materials; the quality of performed preparatory work; software used; management of the construction site, etc. [13-17]. In addition, in construction practice, each of the project participants has their own interests regarding the costs and price of the building.

The factors that influence the costs of the buildings have been investigated by many researchers and participants in the construction processes worldwide, from various aspects [18]. One of the aspects is a research on the factors that determine the costs of a building. Laksono investigated project implementation time, depth of the foundation, number of floors and floor area as independent variables for the multiple linear regression of stepwise method [19]. The contracted value of the project for the building was a dependent variable. Results showed that project time implementation, number of floors and floor areas are factors that have significant influence on building cost.

A guide for detailed estimation of construction costs, based on the estimation by category of works is given in [20]. Similarly, an analysis of the cost structure of construction works is presented in [21]. Authors use the model based on the cost estimation of works.

El-Kholy et al. applied Monte Carlo Simulation for prediction of the simulated cost contingency [22]. For building designs are developed artificial neural network and regression based models to predict simulated cost contingency for steel reinforcement. The research results pointed that the artificial neural network models are more powerful than regression based models in the theoretical modelling of simulated cost contingency.

Design optimization is necessary for each building. Therefore, computational tools play an important role in order to maximize the cost efficiency and the sustainability of the structures. In that sense, [23] presents several iterations for reinforced concrete building layout and develops optimization model that integrates Building information modelling (BIM) with computer programing and structural design. BIM is also used in [24] to present a conceptual cost-estimation model when structural analysis and design are BIM-based.

Data for residential buildings built with reinforced concrete, but damaged due to the earthquake, are analyzed by Del Vecchio et al. [25]. Using computer tools and actual costs for repairing the buildings, authors made probabilistic loss assessments. It was obtained that there are some economic losses in building designs due to their seismic design. Another study [26], analyzed the quantity of structural materials and their estimation for reinforced concrete buildings designed for seismic effects. The conclusion was that the parametric quantity modelling is useful for cost estimation purposes. In that sense, for Indonesia, where earthquakes are often, Suhendi et al. analyzed several types of residential buildings [27]. They noted that for residential buildings the structural costs are average of 34.20% of the total costs.

Related to the construction costs there are useful guides, reports and baselines. They usually give indicative data and guidelines for construction costs, since many factors should be taken into account, according to the specific case [28]. However, the amount of total costs for the building, as a value, do not indicate how the construction costs were distributed and the price was obtained. In that relation, although the estimate cannot be accurate, the benefit of knowing the percentage participation [%] of cost for each type of work in the total construction costs is of great importance, particularly in decisions making processes related to the buildings. There are opportunities to arrange the costs in forms that will be suitable for further use, regardless of the costs variability over time. One such possibility is

determining the cost structure, i.e. determination of the percentage share of the costs of various types of works in the total construction cost.

In RN Macedonia, there is no official data for the costs structure for buildings, nor official methodology and software for costs estimation. Furthermore, it is very difficult to obtain such data from construction companies. Therefore, the aim of this paper is to investigate the cost structure of residential buildings. The focus is on residential buildings with reinforced concrete structural system, as the largest number of constructed buildings for collective housing in RN Macedonia.

2. RESEARCH METHOD

Using interview research method, data have been collected from contractors for fifteen residential buildings built in South-West region of RN Macedonia, in the cities Ohrid and Struga. Buildings are built in the last decade, including all their phases, from their initial period. Their structural system is a reinforced concrete skeleton system built using wooden formwork. Buildings have one underground level and four to seven up-ground levels. Reinforced concrete skeleton systems include vertical columns and walls, as well as horizontal beams in both directions, with various dimensions according to the static calculation. The floor structured are designed as massive reinforced concrete slabs. The basement walls are reinforced concrete, while the facade walls are masonry, with ceramic blocks and energy efficiency facade. Partition walls between the apartments are masonry work of ceramic blocks with appropriate thermal insulation, while the partitions in the apartments are built of plasterboards. The roof structure is timber class 2, with roofing of plasticized ribbed sheet, on a wooden panelling, insulated with mineral wool, protected with a vapour barrier [29].

As mentioned above, there is no official model for costs breakdown and presentation as costs structure in RN Macedonia. Consequently, the contractor and other project participant use their own cost calculation methodology and the selected model for the breakdown of the total building costs and their grouping depends of the contractor's own methodology. Therefore, the buildings' collected data were additionally arranged and grouped in order to be enabled the usage of the same cost structure for all buildings.

3. RESULTS AND DISCUSSION

Nine different groups of works were taken into account in the costs structure of the construction works. That are costs, which have the greatest influence in defining the overall cost for building construction. The nine groups of considered works are earth works, concrete and reinforced-concrete works, masonry works, roofing works, plastering, painting, floor works, insulation works, doors and windows. Their participation in the total building costs was calculated for each building, as well as their average participation (in %) for all buildings.

The costs for preparatory works for each construction site (offices, warehouses, security, water for the construction site, etc.) were not taken into account; they are calculated as a special group of costs that are not analyzed in this paper. The costs of the location are not included, as well.

The results of the performed analysis for each building separately are given in the Table 1. Furthermore, the average value (in percentage [%]) participation of each type of work in the total construction costs was calculated for each building, separately.

Regarding Table 1, the following can be concluded:

- Earth works participate with 2,55-3,60 [%], average 3,02 [%],
- Concrete and Reinforced-concrete works participate with 38,11-44,30 [%], average 41,55 [%],
- Masonry works participate with 9,40-12,28 [%], average 10,84 [%],
- Roofing works participate with 1,93-4,00 [%], average 2,44 [%],
- Plastering participate with 12,38-21,73 [%], average 14,67 [%],
- Painting participate with 0,38-1,02 [%], average 0,76 [%],
- Floor works participate with 10,92-15,10 [%], average 12,95 [%],
- Insulation works participate with 2,47-6,10 [%], average 4,22 [%],
- Doors and windows participate with 8,65-11,38 [%], average 9,55 [%].

The obtained results support the research outputs of Martinec et al. who noted that concrete and reinforced-concrete works has the highest participation in the total costs for buildings with reinforced concrete structure [21]. This is also supported by the research results of Suhendi et al. [27]. As mentioned

above, their research indicates that for residential buildings the concrete structure costs are average of 34.20% of the total costs.

It should be noted that the accuracy of the cost estimation, particularly from the contractor's point of view, depends on a large number of parameters. Some of them are the type of the contract, the quality of the project documentation, applied methods (models) for cost estimation, the personnel in charge of implementing the procedure for estimating costs, the methodology and software used and other factors. Therefore, the presented values are approximate and can be used for roughly prediction of costs for each type of building construction works for residential buildings with reinforced concrete structural system when the building project budget is known.

For the future research is suggested to collect more data and to compare it with the data for constructed residential buildings in other cities and regions in RN Macedonia and, also with the other types of buildings.

Table 1. Construction works participation in total costs for residential buildings

No.	Building gross area [m^2]	Earth works [%]	Concrete and reinforced concrete works [%]	Masonry works [%]	Roofing works [%]	Plastering [%]	Painting [%]	Floor works [%]	Insulation works [%]	Doors and windows [%]
1	3.000,00	2.57	43.63	12.01	1.97	14.99	0.45	11.33	2.82	10.21
2	4.241,40	2.55	42.87	11.46	2.45	13.68	0.42	12.58	3.07	10.91
3	1.617,75	2.57	38.11	9.86	4.00	21.73	0.38	11.27	2.47	9.65
4	2.234.40	3.40	43.10	12.11	1.98	15.26	0.46	10.92	2.57	10.20
5	3.734,37	3.60	42.40	12.28	1.93	15.67	0.49	11.94	2.82	8.87
6	3.282,55	3.05	38.49	11.59	2.03	14.48	0.95	12.56	5.92	10.93
7	3.359,16	3.08	38.89	11.71	2.01	14.31	0.94	12.41	5.85	10.80
8	3.143,50	3.16	38.30	11.64	2.05	14.08	0.94	12.74	5.85	11.38
9	1.826,08	2.89	42.50	9.40	2.20	12.75	0.98	14.52	6.10	8.65
10	1.624,86	3.10	41.46	9.70	2.30	12.38	1.02	15.10	5.80	9.00
11	1586,68	2.90	40.20	9.85	3.35	12.60	1.00	15.10	5.65	9.35
12	2585,30	3.10	41.50	10.15	2.20	15.60	0.90	14.55	2.80	9.15
13	1.326,54	2.95	44.30	10.20	2.80	15.40	1.00	11.50	5.10	6.80
14	935,80	3.00	45.70	9.80	3.30	13.40	0.90	13.65	3.10	7.10
15	2.825,30	3.35	41.80	10.80	2.10	13.70	0.60	14.10	3.40	10.20
Average		3.02	41.55	10.84	2.44	14.67	0.76	12.95	4.22	9.55

5. CONCLUSIONS

Buildings must meet numerous requirements related to relevant regulations, but also from the project participants and future users of the buildings. All this affects construction costs. Therefore, knowing the costs of each type of building work is of particular interest to all project participants.

Cost estimation is an extremely difficult and demanding task, especially in the early phase of the project realization due to the many unknowns in relation to the factors that influence the construction. Accurate cost estimation is not possible. However, the accuracy of cost estimation has an influence on the project realization and project participants' work. The costs presented in this paper are calculated by the contractors of the residential buildings, based on the project documentation for the constructed buildings. Therefore, the values presented are only an indication of how much each type of the building construction work will "roughly" cost. Besides that, the presented values can be used for roughly prediction of costs for works for residential buildings with reinforced concrete structure

The process of development of the cost review is complex and responsible, but it is of great help in all phases of design implementation. Therefore, it is very important to use the experience gained from designs realized up to the moment of the cost estimation. Thus, although the research is focused on building construction in Macedonian context, it can be used as an experience for similar research around the world.

REFERENCES

[1] Awosina, A.; Ndihokubwayo, R.; Fapohunda, J. (2018) “Effects of Inaccurate Cost Estimate on Construction Project Stakeholders,” Journal of Construction Project Management and Innovation, Vol. 8 No 2, pp. 1886-1904.

[2] Car-Pusić, D.; Mlađen, M. (2020), “Early Stage Construction Cost Prediction in Function of Project Sustainability”, Current Topics and Trends on Durability of Building Materials and Components, Serrat, C., Casas, J.R. and Gibert, V. (Eds). 1-8 XV International Conference on Durability of Building Materials and Components, DBMC 2020, Barcelona.

[3] Abdin, Z. N.; Azizi, Z. (2021), “Soft Cost Elements: Exploring Management Components of Project Costs in Green Building Projects,” Environmental Impact Assessment Review, vol. 87, No 106545, 2021. https://doi.org/10.1016/j.eiar.2020.106545

[4] Przesmycka, A.; Wieczorek, D. (2021), “Maintenance Strategies, Periodic Renovations and Building Modernisation in the Aspect of the Criterion of the Whole Life Costs”. Civil and Environmental Engineering Reports. Vol. 31, No 2, pp.15-29, https://doi.org/10.2478/ceer-2021-0017

[5] Solanki, S. K.; Rastogi R.; Paul, V. K. (2022), “Cost Analysis of Functional Retrofitting Measures in Buildings,” Journal of the Institution of Engineers (India): Series A, No 103, pp. 725–732.

[6] Cecconi, R. F.; Moretti, N.; Dejaco, C. M. (2019), “A Bibliometric Analysis on Costs Estimation of Building Retrofit,” IOP Conference Series Earth and Environmental Science, Vol. 290, No 012136.

[7] Haider, U.; Khan, U.; Nazir, A.; Humayon, M. (2020), “Cost Comparison of a Building Project by Manual and BIM,” Civil Engineering Journal. Vol. 6, No 1, pp. 34-49, http://dx.doi.org/10.28991/cej-2020-03091451

[8] Hu, M.; Skibniewski, J. M. (2021a), “Green Building Construction Cost Surcharge: An Overview,” Journal of Architectural Engineering. Vol. 27, No 4, 4021034. https://doi.org/10.1061/(ASCE)AE.1943-5568.0000506

[9] Hu, M.; Skibniewski, J. M. (2021b), “View of a Review of Building Construction Cost Research Current Status, Gaps and Green Buildings,” Construction Economics and Building, Vol. 2, No 1, pp. 1-17. https://doi.org/10.37256/gbce.212021768

[10] Wibowo, P. W.; Witjaksana, B.; TJendan, T. H. (2023), “Analysis of Contract Change Order (CCO) Costs in Building Construction Projects.” Asian Journal of Engineering, Social and Health, Vol. 2, No 12, pp. 1720-1732, doi:https://doi.org/10.46799/ajesh.v2i12.211

[11] Altan, M.F.; Çakir, S. (2025), “Project and cost management in construction projects”. TAS Journal/Journal of Technical and Applied Sciences, Vol. 5 No. 1, pp. 1-14. doi: https://doi.org/10.5281/zenodo.15308596

[12] Mohammad Waffy, F.; Chia-Kuang, L.; Puteri, M.T. (2021), “Cost estimation performance in the construction projects: A systematic review and future directions”. International Journal of Industrial Management, Vol. 11, pp. 217-234,

[13] Elserougy, M.; Khodeir, L. M.; Fathy, F. (2024), “Practices and Techniques for Construction Projects Cost Control - A Critical Review,” HBRC Journal. Vol. 20, No 1, pp. 525–552. https://doi.org/10.1080/16874048.2024.2337060

[14] Ajayi, T. O.; Daramola, O. T., Adhuze, O. O. (2024). "Cost Management Evolution in Building Projects: A Review of Innovations and Challenges", International Journal of Research and Innovation in Applied Science, vol. IX, No IX, pp. 80-95. doi: 10.51584/IJRIAS.2024.909009

[15] Memon, H.A.; Rahman, A.I.; Aziz, A.A.A.; Kumarason V.R.; Hanas, I.M.N. (2011), “Identifying Construction Resource Factors Affecting Construction Cost: Case of Johor”. Malaysian Technical Universities International Conference on Engineering & Technology (MUiCET-2011). pp. 1-10.

[16] Tayefeh Hashemi, S.; Ebadati, O. M.; Kaur, H. (2020), “Cost Estimation and Prediction in Construction Projects: A Systematic Review on Machine Learning Techniques,” SN Applied Sciences, Vol. 2, Art. no. 1703. https://doi.org/10.1007/s42452-020-03497-1

[17] Pham, T. Q. D.; Le-Hong, T.; Tran, V. X. (2023), “Efficient Estimation and Optimization of Building Costs Using Machine Learning,” International Journal of Construction Management. Vol. 23, No 5, pp. 909-921. https://doi.org/10.1080/15623599.2021.1943630

[18] Ali, B.A.; Rahman, H.M. (2019), “A Study on Estimation and Costing of a Seven Storied Residential Building in Dhaka City”. Journal of Structural Engineering, its Applications and Analysis. Vol. 2 No. 3, pp. 1-8.

[19] Laksono, D. T. (2017), “The Analysis of the Factors Which Affect the Building Costs in Indonesia.” Civil Engineering Journal. Vol. 3, No 1, pp. 57-62, 2017.

[20] Chee H.F. (2019), “Pitfalls in Solving Affordable Housing Issue”. Asian Property Review – Investment. Vol. September, pp. 38-42. Available at: https://www.researchgate.net/publication/335650924_Pitfalls_in_Solving_Affordable_Housing_Issue (accessed December 2025).

[21] Martinec, N.; Ajduković Hrnjak, N.; Bezak, S. (2010), “Struktura troškova građevinskih radova u visokogradnji”. Gradevinar, Vol. 62, No. 4, pp. 307-311.

[22] El-Kholy, A. M., Tahwia, A. M., & Elsayed, M. M. (2020), “Prediction of simulated cost contingency for steel reinforcement in building projects: ANN versus regression-based models”. International Journal of Construction

Management, Vol. 22 No. 9 pp. 1675–1689. https://doi.org/10.1080/15623599.2020.1741492

[23] Sherif, M.; Nassar, K.; Hosny, O.; Safar, S.; Abotaleb, I. (2022), “Automated BIM-based structural design and cost optimization model for reinforced concrete buildings”. Scientific Reports, Vol. 12, Article No. 21616

[24] Wu, C.L.; Wang K.C.; Wang W.C. (2018), “A BIM-based Conceptual Cost Estimation Model Considering Structural Analysis and Design”, Proceedings of the 35th ISARC, Berlin, Germany, pp. 278-285.

[25] Del Vecchio, C.; Ludovico, M.D.; Prota, A. (2020), “Repair costs of reinforced concrete building components: from actual data analysis to calibrated consequence functions.” Earthquake Spectra, Vol. 36 No 1, pp. 353-377. https://doi.org/10.1177/8755293019878194

[26] Thiruvengadam, V.; Guite, T.; Thakre, R.K.; Wason, J.C. (2018), Quantity Estimation of Structural Materials in Reinforced Concrete Buildings Designed for Seismic effects, June 2018, Conference: 16 European Conference on Earthquake Engineering, Greece, pp 1-12.

[27] Suhendi, C.; Fadjri Kusumah, M.; Priatman, F.; Ferdiansyah, F. (2024), “The Percentage of Structural Costs in Houses Structured Type 30, 36, 45 and 70 with Houses with Simple Structures.” Proceedings of the international conference on consumer technology and engineering innovation (ICONTENTION 2023), pp. 135-143. https://doi.org/10.2991/978-94-6463-406-8_24

[28] Kermanshachi, S.; Safapour, E.; Anderson, S.; Molenaar, K.R.; Schexnayder, C. (2018) “Development of the Cost Baseline for Achieving Excellence in Rural Transit Facilities” Conference: Transportation Research Board 98th Annual Conference.

[29] Ajdinoski, E. (2023), “Cost structure of construction works on residential-business buildings”. Master Thesis, UKIM, Faculty of Civil engineering, Skopje (in Macedonian).

VALIDATION OF ENERGY SIMULATION MODELS THROUGH COMPARISON WITH ACTUAL ENERGY CONSUMPTION IN BUILDINGS

Liljana Dimevska Sofronievska
MSc, Teaching Assistant
Ss. Cyril and Methodius University in Skopje
Faculty of Architecture
North Macedonia
dimevska.liljana@arh.ukim.edu.mk
0009-0000-4585-6951

Dobre Nikolovski
PhD, Associate Professor
Ss. Cyril and Methodius University in Skopje
Faculty of Architecture
North Macedonia

Bojan Karanakov
PhD, Professor
Ss. Cyril and Methodius University in Skopje
Faculty of Architecture
North Macedonia
0000-0003-3026-6769

Received: 01.12.2025
Accepted: 22.01.2026
Published: 25.01.2026

DOI: 10.55302/SJCE2514237ds

This paper examines the application of computer-based energy modeling and simulation tools in the analysis of building energy performance. The research is based on a comparative case study of two buildings, where detailed 3D models and energy simulations were developed using real data on construction systems, materials, heating, cooling and ventilation systems, as well as local climatic conditions.

The simulation results were compared with the actual energy consumption data for thermal and electrical energy on both monthly and annual levels. The analysis indicates a high level of agreement between simulated and measured values (over 90%), confirming the accuracy and reliability of the applied methodology. In addition to energy consumption, the simulations provide detailed insight into the thermal behavior of the buildings, including heat losses and gains, envelope performance, and CO_2 emissions.

The findings demonstrate that energy simulation tools represent an effective approach for analyzing, evaluating, and improving building energy performance, with significant potential for application in both research and engineering practice.

Keywords: energy simulation, building energy performance analysis, 3D modeling, energy consumption.

Scientific Journal of Civil Engineering (SJCE)
© 2025 by Faculty of Civil Engineering, SCMU - Skopje is licensed under CC BY-SA 4.0

1. INTRODUCTION

Computer graphics and digital modeling technologies have become essential tools in contemporary architectural design, enabling faster project development, improved decision-

making processes, and realistic visualization of architectural solutions. The continuous advancement of digital technologies has significantly transformed the architecture, engineering, and construction (AEC) industry, particularly through the introduction of Building Information Modeling (BIM). BIM provides comprehensive digital representations of buildings and facilitates data exchange throughout the entire building lifecycle, from conceptual design to operation and maintenance [1].

In addition to supporting the design process, BIM-based models serve as a foundation for advanced building performance analyses. However, BIM alone is not sufficient for evaluating the actual energy behavior of buildings under real operating conditions. Accurate assessment of energy performance requires the use of dynamic simulation tools capable of modeling heat transfer processes, energy consumption patterns, HVAC system operation, occupant behavior, and climatic influences. Software platforms such as DesignBuilder and EnergyPlus have therefore become widely used for predicting building energy performance and supporting energy-efficient design strategies.

Previous studies have demonstrated that building energy simulation tools can provide reliable estimates of energy demand and thermal performance. Nevertheless, differences between simulated and measured energy consumption are frequently reported due to uncertainties associated with material properties, occupancy schedules, equipment usage, climatic conditions, and system operation. Consequently, the validation of simulation models through comparison with actual energy consumption data remains an important research topic, particularly for improving the reliability of energy performance assessments.

The objective of this study is to evaluate the accuracy and applicability of building energy simulation models through a comparative analysis of simulated and measured energy consumption data. Two existing buildings with different architectural and construction characteristics were selected as case studies in order to assess the reliability of simulation results under varying building conditions. Detailed virtual models of both buildings were developed using DesignBuilder software with the EnergyPlus simulation engine. The modeling process included the definition of building geometry, construction materials, thermal envelope characteristics, HVAC systems, occupancy patterns, and local climatic conditions. The simulation results were subsequently compared with actual energy consumption data to evaluate the accuracy of the developed models and their applicability for energy-efficiency assessments and future building performance analyses..

2. METODOLOGY

This study applies a comparative simulation-based methodology for the evaluation and validation of building energy performance through the use of dynamic thermal simulations. The approach is based on the development of detailed digital models of two existing buildings and the comparison of simulated energy consumption with measured operational data. The methodological framework consists of the following steps: collection of architectural and technical documentation for both buildings, on-site verification of geometrical and construction characteristics, development of detailed 3D thermal models, definition of building envelope properties, internal loads, HVAC systems, and operational schedules, dynamic energy simulation, and comparison and validation of results against measured energy consumption data.

2.1 CASE STUDY BUILDINGS

Two existing buildings with different geometrical, structural, and functional characteristics were selected in order to evaluate the reliability of simulation models under different operational conditions. For each building, geometric data, construction details, and operational characteristics were collected from project documentation and field surveys. The buildings were modeled as separate thermal zones according to their functional layout, orientation, and usage patterns.

2.2 DEVELOPMENT OF SIMULATION MODELS

Three-dimensional models of both buildings were developed using DesignBuilder, while EnergyPlus was used as the simulation engine for dynamic thermal calculations. The following input data were defined for each building model: Building geometry and zoning configuration; Construction assemblies of external and internal envelope elements; Thermo-physical properties of materials (thermal conductivity, density, specific heat capacity, and U-values); Window systems, glazing properties, and shading elements; Air

infiltration rates and ventilation assumptions; Internal heat gains (occupancy, lighting, and equipment loads); HVAC system configuration and operational schedules. Where available, real operational data were used to define realistic usage profiles in order to improve model accuracy.

2.3 CLIMATIC DATA

Weather data were obtained from a representative EnergyPlus Weather (EPW) file corresponding to the geographical location of the studied buildings. Hourly climatic parameters including outdoor temperature, solar radiation, humidity, and wind speed were used as input for the simulations.

2.4 SIMULATION AND VALIDATION PROCEDURE

Dynamic energy simulations were performed using EnergyPlus through the DesignBuilder interface. The simulations were conducted on an hourly basis over a full annual cycle. The validation of the developed models was performed by comparing simulated energy consumption with measured energy data obtained from utility bills and/or building monitoring records. The comparison focused on: annual heating energy consumption; Total building energy use; Seasonal variation of energy demand. Differences between simulated and measured results were analyzed in order to identify uncertainties related to occupancy behavior, system efficiency, material properties, and operational conditions.

This methodology enables assessment of model accuracy and provides a reliable basis for evaluating the applicability of building energy simulation tools in real operational conditions.

3. SIMULATIONS

3.1 SELECTION OF CASE STUDIES

The analysis of energy performance was conducted through two case studies selected as representative examples of modernist architecture in Skopje, characterized by complex spatial and functional configurations. The first building is the headquarters of the Macedonian Academy of Sciences and Arts (MASA), constructed in the 1970s, which represents a protected cultural heritage asset of the first category. The second building is the administrative building of the State Hydrometeorological Service in Skopje, also constructed in the same period and in a similar architectural style, representing a unique complex composition of multiple volumes and distinctive cylindrical towers. This building has also been proposed for protection as a cultural heritage asset of the second category.

Both buildings were constructed entirely in exposed concrete, without the application of thermal insulation, which is characteristic of the architectural practice of that period. These structural and material characteristics, combined with the ageing and degradation of materials over time, lead to pronounced issues related to energy efficiency, thermal comfort, and long-term sustainability. Consequently, they represent a relevant basis for conducting detailed energy simulations and analyzing their performance under real operational conditions. The buildings are shown in Fig. 1 and Fig. 2.



Figure 1. Case Study 1: Macedonian Academy of Sciences and Arts



Figure 2. Case Study 2: Hydrometeorological Institute

The selection of the two case study buildings was based on their representative characteristics within the local building stock and their relevance for energy performance assessment. Although the buildings differ in geometry, architectural configuration, construction period, and material composition, this variation was intentionally used to evaluate the robustness of building energy simulation models under different conditions. The main selection criterion was the availability of complete architectural documentation,

construction data, and measured energy consumption records required for reliable model development and validation. The differences between the two buildings enable a comparative assessment of simulation accuracy across different building typologies, providing a broader validation of the modeling approach. The buildings are therefore not intended to be identical, but to serve as contrasting case studies for evaluating simulation performance under varying geometrical and thermal conditions. This approach improves the reliability of the results and enhances the applicability of the findings to a wider range of existing buildings.

3.2 GEOMETRY, LOCATION, ZONING, AND DESIGN TEMPERATURE

Case study 1 is a free-standing institutional structure located in a dense urban context and exposed to external conditions on all façades. The building is characterised by a relatively compact but thermally inefficient geometry dominated by large glazed surfaces and reinforced concrete volumes. The internal layout is divided into a high number of thermal zones exceeding 250 zones, where each room is defined as an individual thermal zone due to variations in occupancy, orientation, and internal gains. The building includes offices, laboratories, auditoriums, and service spaces distributed across multiple levels.

Case study 2 is a larger and more complex institutional facility with a multifunctional program and an atrium-based spatial organisation. The geometry is significantly more heterogeneous, including a main volume and a later administrative extension that introduces an internal courtyard configuration. The building is divided into approximately 257 thermal zones, reflecting its highly fragmented functional layout. Zones include administrative offices, libraries, archives, conference halls, exhibition spaces, and service areas, each with different occupancy schedules and internal loads.

For both buildings, design temperature conditions are defined based on local hourly climate data, with dynamic external temperature variation applied throughout the simulation period. The internal organization is addressed through detailed zoning, whereby each space is modelled as a separate thermal zone. This approach is derived from differences in function and usage patterns, which vary according to occupancy levels, equipment, lighting, orientation, and conditioning regimes. A specific design temperature is assigned to each zone, enabling a more accurate simulation of real operating conditions. The zoning approach is illustrated in Fig. 3 and Fig. 4.



Figure 3. Thermal Zones – Case Study 1

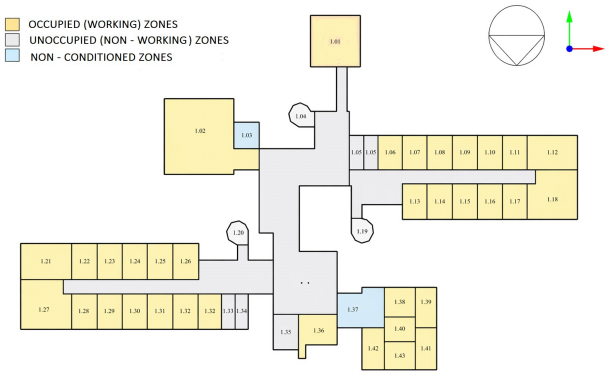


Figure 4. Thermal Zones – Case Study 2

Figures 3 and 4 illustrate the method of zoning the space into thermal zones, defined according to the functional use of the rooms. This approach is applied identically in both analysed buildings. Based on functional purpose, the following groups of thermal zones are distinguished:

Occupied (working) zones – spaces with continuous user presence, in which heating, cooling, and appropriate ventilation are provided in accordance with external climatic conditions (offices, laboratories, meeting rooms, galleries, auditoriums, etc.); Unoccupied zones – spaces not intended for permanent human occupancy, but which are heated during the heating season (corridors, hallways, etc.); Unheated / non-conditioned zones – spaces without permanent occupancy that are not subject to thermal conditioning, i.e.,

they are neither heated nor cooled (staircases, toilets, storage rooms, etc.). The zoning principle is consistently applied across all floors, including basement levels, and is identical for both buildings. Although in Figure 2 the zones are presented as groups with similar functions and thermal requirements, in the model they are considered as separate individual thermal zones. The design indoor temperature for occupied working zones (offices, halls, amphitheatres, etc.) is 21°C, while for unoccupied zones (corridors, toilets, and basement spaces) a temperature of 15°C is assumed. The number of users is significantly higher in occupied zones compared to unoccupied ones. Additionally, parameters such as orientation, spatial position, floor level, adjacency to other zones, and exposure to external influences vary for each zone and change dynamically during the simulation. The outdoor temperature also varies according to real climatic data, which are taken into account in the simulation process.

3.3 HEATING, COOLING, AND VENTILATION SYSTEMS

Case study 1 is equipped with a centralized hydronic HVAC system connected to district heating for space heating. Heat distribution is provided via fan-coil units installed in all conditioned spaces, while radiators are used in service zones such as corridors and toilets. Cooling is provided through a centralized chiller system with chilled water temperatures between 7–12°C. Mechanical ventilation is very limited and primarily restricted to sanitary spaces, resulting in dominant reliance on natural ventilation and infiltration. Due to poor envelope performance, the building frequently requires supplementary electric heating and split-unit air conditioning, particularly during winter and summer peak conditions.

Case study 2 has a more advanced but still partially inefficient HVAC configuration. Heating is also connected to a district heating system with secondary heat exchange delivering water at approximately 70–80°C. Cooling is provided through centralized chillers integrated with fan-coil systems. In addition, Building 2 includes mechanical ventilation with heat recovery in selected high-occupancy zones such as auditoriums, conference halls, libraries, archives, and exhibition spaces, with estimated heat recovery efficiency in the range of 50–70%. Remaining zones rely on natural ventilation and mechanical exhaust systems. Despite this more advanced configuration, the building still exhibits high energy demand due to envelope limitations and infiltration losses.

3.4 CONSTRUCTION AND ENVELOPE MATERIALS

Building 1 is constructed as a reinforced concrete frame structure with exposed concrete façades and extensive use of single-glazed aluminium curtain wall systems. The building has no continuous thermal insulation in the original construction. External walls exhibit very high thermal transmittance, with U-values ranging from approximately 1.73 W/m²K to 5.08 W/m²K, depending on wall typology. Roof structures include flat reinforced concrete slabs with limited insulation performance, with U-values between 0.44 W/m²K and 1.69 W/m²K. Ground-related slabs and intermediate floors show U-values in the range of 2.17–4.21 W/m²K, indicating significant heat transfer to unconditioned zones. Window systems are highly inefficient, with U-values up to 5.78 W/m²K, representing the weakest component of the envelope.

Building 2 is also based on reinforced concrete structural systems, but includes multiple construction phases. The original part of the building is largely uninsulated, while the later extension incorporates approximately 5 cm of internal thermal insulation. External wall U-values vary between 0.54 W/m²K and 4.68 W/m²K, depending on construction type and period. Roof assemblies show improved performance compared to Building 1, with U-values ranging from 0.28 W/m²K to 0.42 W/m²K, due to partial insulation layers. Ground floor and slab elements present U-values between 0.99 W/m²K and 1.98 W/m²K. Window systems include a combination of single and improved glazing, with U-values ranging from 2.0 W/m²K to 5.61 W/m²K, depending on the façade zone and construction phase.

.4. RESULTS

Based on the conducted modelling and simulation of the existing conditions for both buildings, a set of relevant output parameters was obtained, encompassing their energy and thermal performance. In this regard, the analysis includes the consumption of thermal and electrical energy (for heating, cooling, ventilation, lighting, and equipment), CO_2 emissions, as well as internal microclimatic conditions (temperature and relative humidity) across individual thermal zones. In addition, heat losses through the building envelope, infiltration, and ventilation were examined,

along with the thermal characteristics of the construction elements expressed through their U-values.

From the obtained results, parameters relevant for model verification were extracted, which are comparable with the actual consumption of thermal and electrical energy. These were systematized and presented graphically in order to enable a comparative analysis with the measured data obtained from energy bills. In order to determine the accuracy and validity of the applied software model, comparative analyses were carried out between the actual energy consumption for heating, cooling, and operation—derived from monthly thermal and electrical energy bills over a one-year period—and the results of the simulated existing conditions obtained through a 3D model and energy simulation of both buildings. The analyses are graphically presented in Figures 5, 6, 7, and 8.

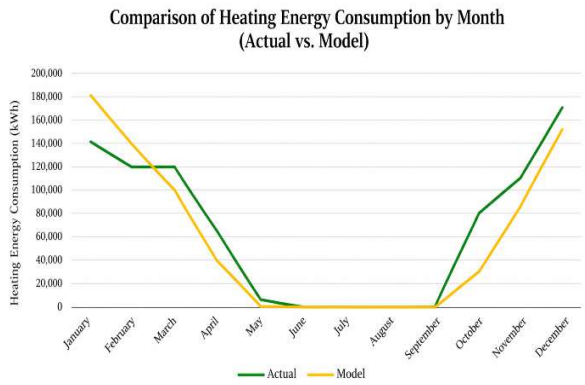


Figure 5. Heating energy consumption (comparison of utility bills and model results) – Case Study 1

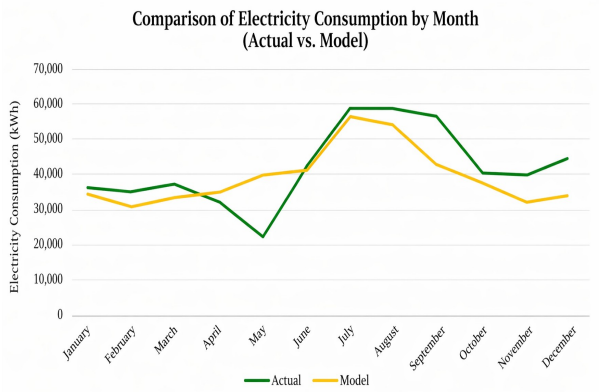


Figure 6. Electricity consumption (comparison of bills and model results) – Case Study 1

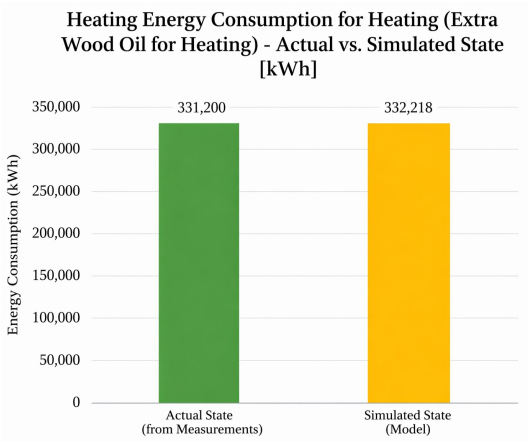


Figure 7. Heating energy consumption (comparison of utility bills and model results) – Case Study 2

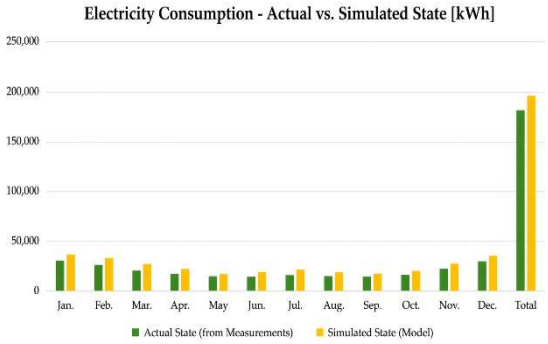


Figure 8. Electricity consumption (comparison of bills and model results) – Case Study 2

The obtained results indicate a high level of agreement between the actual and simulated values, confirming the reliability and applicability of the model. As shown in Figures 5 and 6, which present the comparison of thermal energy consumption, a correspondence exceeding 90% is observed at both the monthly and total levels, further validating the accuracy of the performed simulation.

5. CONCLUSION

The aim of this research is to highlight the role and significance of computer-based software tools in architecture and civil engineering, particularly in the domain of complex energy analyses and the prediction of building performance under real operating conditions. To this end, detailed 3D models were developed and energy simulations were conducted for the two analyzed buildings, based on comprehensive research, documentation, and systematization of relevant input data.

The modelling process involved the precise definition of geometry, materials, structural characteristics, heating, cooling, and ventilation systems, as well as local climatic conditions and the surrounding urban context. The application of advanced software tools enabled a realistic simulation of energy performance under dynamic (non-steady-state) conditions and the generation of detailed hourly results.

The simulation outputs were compared with actual data obtained from thermal and electrical energy consumption bills, revealing a high level of agreement (exceeding 90%) for both buildings. This strong correspondence confirms the accuracy, reliability, and practical applicability of the employed methodology and software tools.

In addition to energy consumption, the simulations provide detailed insight into the thermal behavior of the buildings, including heat losses and gains, the influence of the building envelope, and associated greenhouse gas emissions. Such an approach represents a solid foundation for further analyses and the development of improvement scenarios aimed at enhancing energy efficiency, sustainability, and overall building performance.

Based on the obtained results, it can be concluded that the application of computer-based simulations represents a robust and effective tool for analyzing and improving building energy performance, with significant potential for application in future research as well as in practical engineering and architectural interventions.

REFERENCES

[1] Azhar, S. (2011) Building Information Modelling (BIM): Trends, Benefits, Risks, and Challenges for the AEC Industry. Leadership and Management in Engineering, 11(3), July 2011.

[2] Corrado, V., & Fabrizio, E. (2019) Steady-State and Dynamic Codes: Critical Review, Advantages and Disadvantages, Accuracy, and Reliability. In: Handbook of Energy Efficiency in Buildings, 2019

[3] Hossain, Md. F. (2019). Sustainable Design and Build: Building, Energy, Roads, Bridges, Water and Sewer Systems. Advanced Building Design, pp. 137–230

[4] U.S. Department of Energy (2022) EnergyPlus™ Version 22.2.0 Documentation: Getting Started. September 28, 2022

[5] Gasparella, A., & Pernigotto, G. (2012) Extensive Comparative Analysis of Two Building Energy Simulation Codes for Southern Europe Climates: Heating and Cooling Energy Needs and Peak Loads Calculation in TRNSYS and EnergyPlus. II International High Performance Buildings Conference, West Lafayette, Indiana, USA

[6] Rallapalli, S. H. (2010) A Comparison of EnergyPlus and eQUEST Whole Building Energy Simulation Results for a Medium Sized Office Building. Master of Science Thesis

[7] Dandan, Z., et al. (2013) A Detailed Loads Comparison of Three Building Energy Modelling Programs: EnergyPlus, DeST and DOE-2.1E. Building Simulation, 6(3), pp. 324–335

[8] Sousa, J. R. B. (2012) Energy Simulation Software for Buildings: Review and Comparison. Engineering, Computer Science. Available at: https://api.semanticscholar.org/CorpusID:7593404

[9] DesignBuilder. (2023) DesignBuilder Dynamic Simulation Model User Manual (DSM v7.2.0)